

Frequency adaptation in controlled stochastic resonance utilizing delayed feedback method: Two-pole approximation for response function

Hiroki Tutu*

Department of Applied Analysis and Complex Dynamical Systems, Graduate School of Informatics, Kyoto University, Kyoto 606-8501, Japan

(Received 23 December 2010; published 7 June 2011)

Stochastic resonance (SR) enhanced by time-delayed feedback control is studied. The system in the absence of control is described by a Langevin equation for a bistable system, and possesses a usual SR response. The control with the feedback loop, the delay time of which equals to one-half of the period ($2\pi/\Omega$) of the input signal, gives rise to a noise-induced oscillatory switching cycle between two states in the output time series, while its average frequency is just smaller than Ω in a small noise regime. As the noise intensity D approaches an appropriate level, the noise constructively works to adapt the frequency of the switching cycle to Ω , and this changes the dynamics into a state wherein the phase of the output signal is entrained to that of the input signal from its phase slipped state. The behavior is characterized by power loss of the external signal or response function. This paper deals with the response function based on a dichotomic model. A method of delay-coordinate series expansion, which reduces a non-Markovian transition probability flux to a series of memory fluxes on a discrete delay-coordinate system, is proposed. Its primitive implementation suggests that the method can be a potential tool for a systematic analysis of SR phenomenon with delayed feedback loop. We show that a D -dependent behavior of poles of a finite Laplace transform of the response function qualitatively characterizes the structure of the power loss, and we also show analytical results for the correlation function and the power spectral density.

DOI: [10.1103/PhysRevE.83.061106](https://doi.org/10.1103/PhysRevE.83.061106)

PACS number(s): 05.40.Ca, 02.30.Ks

I. INTRODUCTION

Noise-induced phenomena in nonlinear dynamics have been widely studied [1–10]. Stochastic resonance (SR) [1–6] and coherent resonance (CR) [7–10] are the prominent examples of such phenomena. SR is the phenomenon where the response of system to input signal is improved by an appropriate amount of noise. CR is the phenomenon found in excitable systems in the context of chemical oscillation or neural network systems where the system manifests a coherent oscillation as an appropriate amount of noise is supplemented.

In recent years, noise-induced phenomena where delayed feedback loop and noise constructively work to enhance a coherence of response is a subject of great interest [11–18]. Misono *et al.* reported in Refs. [19,20] a noise-induced phase-locking phenomenon in a Schmitt-trigger inverter with delayed feedback loop in which, as a noise intensity reaches an appropriate level, the frequency of oscillation induced by CR approaches to that of external signal, and this causes a resonance. One of the characteristics in such SR in systems with delays is bimodal or multimodal peaks at different noise intensities in a signal-to-noise-ratio measure on power spectral density of output time series or coherence measure [20,21]. Such phenomena with multiple resonances at different noise intensities have also been reported in mathematical models [22,23] in the contexts of neural network system or chemical oscillation since the first experimental study in the Belousov-Zhabotinsky reaction system by Miyakawa *et al.* [21,24].

Although relevance of such SR with delayed feedback loop to neural networks or animal sensory systems is often emphasized, mathematical tools for analyzing such phenomena are still in infancy because of difficulties from

non-Markovian property. SR can be characterized by a response function that describes a relationship between input and output signals, and which is obtained from a conditional probability function (CPF). Let $P(\mathcal{X}, t | \mathcal{X}', t')$ be a CPF for finding a state $X(t) \in \mathcal{X}$ at a time t under the condition $X(t') \in \mathcal{X}'$ at t' , where $X(t)$ is a stochastic variable, \mathcal{X} and \mathcal{X}' are sets of state. In general, the nature of non-Markovian systems is that a master equation for $P(\mathcal{X}, t | \mathcal{X}', t')$ may depend on more highly CPF, e.g., that with multiple conditions $P(\mathcal{X}, t | \mathcal{X}', t'; \mathcal{X}'', t'')$, and this causes most of the difficulties. Usually, theoretical treatment employs some kind of approximation to reduce such a non-Markov-type master equation to a Markov one. In some cases, moreover, some kind of self-consistent approximation may be required to obtain a closed set of equations for the CPF.

An earlier theoretical study on CR (or SR) in a bistable system with a delayed input has been carried out in Ref. [12]. The study [12] provides a framework to deal with correlation function and response function on the basis of the dichotomic model [5,6], which is the basic model of SR even in non-Markovian systems. Several extensive studies follow this study (see, e.g., Refs. [25,26]). However, in these studies, the CPF is somewhat oversimplified; then, for a more self-consistent and systematic treatment, an extension taking a property of the CPF into account should be added to these studies. Small time-delay approximation also provides a useful tool for analyzing SR or CR induced by time delay [27,28]. It can be said that the approximation makes the non-Markovian system into an effective Markovian system with a modified potential function through the Taylor series expansion of delay term. And, this gives a successful explanation for the multiple resonances mentioned above in a small delay case [18,29]. In this approach the problem of the CPF is removed; however, there is a certain necessity to understand the non-Markovian nature with the CPF without expanding it to the differential series.

*tutu@acs.i.kyoto-u.ac.jp

In a previous paper [30], the author studied SR in a theoretical model for a bistable magnetic system that is designed to enhance the coherence of SR utilizing a time-delayed feedback control. As mentioned above, in this system, the power loss exhibits two peaks at different noise levels. However, the theory for the power loss was incomplete because of some *ad hoc* assumptions employed, and the theory for the correlation function was not obtained. In this paper, we show a more refined analysis, which is based on the treatment in Ref. [12] and additionally incorporates what we call delay-coordinate series expansion for response function. It is a method to expand a non-Markovian transition probability flux to memory fluxes on a discrete delay-coordinate system, the form of which may be reminiscent of the memory term in the Mori-Zwanzig formalism [31,32]. In the studies mentioned above, this type of approach has not been examined. In this approach, the M th order series expansion of response function on the delay-coordinate system yields $2M$ poles in its finite Laplace transform, and we also call it $2M$ -pole expansion (approximation). This study shows the results of the power loss, the correlation function, and the power spectral density obtained from its primitive implementation, i.e., the two-pole expansion. The obtained results imply that the method can be a potential tool for a systematic analysis of the SR phenomenon with delayed feedback loop. One noticeable point is that the noise-dependent behavior of the pole gives an important characteristic for SR and has a close relationship with the shape of the power loss. A second point is that the linear response relation [33] between a signal input and an output can not hold in a similar way as that of the conventional SR in the Markovian system, but it has an additive input term due to a coherence induced by interplay between noise and the time-delayed feedback loop.

This paper is organized as follows. In Sec. II, we introduce a model described by the Langevin equation and the corresponding Fokker-Planck equation. In Sec. III, we review the feature of the SR. In Sec. IV, we obtain a master equation for a dichotomic model. In Sec. V, we obtain the response function on the basis of the two-pole expansion. Section VI gives tests for the analytical results for the power loss and its related quantiles, correlation function, and power spectral density. The last section summarizes the whole results.

II. MODEL

A. Langevin equation

Let us consider a controlled system that induces SR for an ac input signal. Let $X \equiv X(t)$ be a scalar variable at a time t , and let us assume that it obeys the Langevin equation

$$\dot{X} = -V'(X) + H_{ac}(t) + H_{fb}(t) + R(t), \quad (2.1)$$

where $V'(X) \equiv dV(X)/dX$, $V(X) = (1 - X^2)^2/4$, and $H_{ac}(t) = h \cos(\Omega t)$ is the ac input signal with the amplitude h and the (angular) frequency Ω ($2\pi/\Omega \equiv T$). $H_{fb}(t)$ is a time-delayed feedback control (TDFC) given by

$$H_{fb}(t) = -K \{X(t) + X(t - \tau)\}, \quad (2.2)$$

where K is a feedback gain and the delay τ is chosen as $\tau = \pi/\Omega = T/2$ (the half-period delayed feedback [34]). $R(t)$ is a Gaussian white noise satisfying $\langle R(t) \rangle = 0$ and

$$\langle R(t)R(t') \rangle = 2D\delta(t - t'), \quad (2.3)$$

where $\langle \dots \rangle$ denotes the average over the whole stochastic process.

The potential function $V(X)$ has two local minima at $X = 1$ and -1 . The model for the case $K = 0$ is used as a fundamental model for SR. In that case, the SR occurs in the case that the mean switching rate (Kramers rate) between two states $X > 0$ and $X < 0$ in the absence of $H_{ac}(t)$ and $H_{fb}(t)$, $\tilde{w}_K \sim e^{-1/(4D)}$, satisfies the relationship $\tilde{w}_K \sim \Omega$ [5,6]. The TDFC [Eq. (2.2)] is designed to enhance the coherence of the SR. Namely, the system possesses the reflection symmetry due to the invariance of the system for $X \rightarrow -X$ and $t \rightarrow t - \pi/\Omega$, and the TDFC works for regulating the output to a symmetric oscillatory cycle satisfying $X(t) = -X(t - \pi/\Omega)$. Actually, as an appropriate amount of noise is supplemented, the time-delayed feedback loop gains a potential to induce an oscillatory switching cycle between the two states in accordance with the symmetry mentioned above. Although such a symmetric oscillatory cycle may be allowed for the cases $\tau = n\pi/\Omega$ ($n = 3, 5, \dots$), we limit ourselves to the case $n = 1$. For more information about several utilities of TDFC, see Ref. [35].

B. Fokker-Planck equation

The Fokker-Planck equation (FPE) corresponding to Eqs. (2.1)–(2.3) is given as follows. For a general derivation of FPE from a Langevin equation with the time delay, see Refs. [27,36,37]. Let $p(x, t|\cdot)dx$ be a conditional probability for $X(t) \in [x, x + dx]$, where the “dot” stands for condition(s). A typical condition is that a constraint $X(t') = x'$ at a given time t' , i.e., $p(x, t|x', t')$, or an initial process $\{X(t)| - \tau \leq t \leq 0\} [\equiv \{x\}_i]$, i.e., $p(x, t|\{x\}_i)$. Then, the conditional probability density function (CPDF) $p(x, t|\cdot) (\equiv p)$ obeys

$$\frac{\partial}{\partial t} p = -\frac{\partial}{\partial x} \mathcal{J}, \quad \mathcal{J} \equiv F(x, t|\cdot)p - D\frac{\partial}{\partial x} p, \quad (2.4)$$

where

$$F(x, t|\cdot) \equiv -V'(x) + H_{ac}(t) - K(x + \langle x_\tau | x, t; \cdot \rangle), \quad (2.5)$$

$$\langle x_\tau | x, t; \cdot \rangle \equiv \int_{-\infty}^{\infty} dx_\tau x_\tau p(x_\tau, t - \tau | x, t; \cdot). \quad (2.6)$$

$\langle x_\tau | x, t; \cdot \rangle$ denotes the conditional average for the condition “ $X(t) = x$ ” at the time t and some additional one, which inherits from the CPDF $p(x, t|\cdot)$. Let $p(x_\tau, t - \tau; x, t|\cdot)$ be the conditional joint probability density function (CJPDP) for the jointed states $x = X(t)$ and $x_\tau = X(t - \tau)$ at the times t and $t - \tau$, which depends on the same condition(s) as the CPDF. Then, the CJPDP and the CPDF $p(x_\tau, t - \tau | x, t; \cdot)$ in Eq. (2.6) have a relationship

$$p(x_\tau, t - \tau | x, t; \cdot) = p(x, t; x_\tau, t - \tau | \cdot) / p(x, t|\cdot). \quad (2.7)$$

As shown here, the FPE depends on the CPDF or the CJPDP, which involves a more higher order correlation effect. One of

the subjects in the later analysis is to reduce this complexity without losing the essence of the correlation effect.

III. CHARACTERISTICS OF SR

In this section, we provide an overview of the characteristic features of SR in the present model, employing the power loss defined as follows. The mean work done by the field (signal) $H_{ac}(t)$ during a period T_{tot} is defined as

$$P_{ac} \equiv \frac{1}{T_{tot}} \int_0^{T_{tot}} dt \dot{X}(t) H_{ac}(t). \quad (3.1)$$

This is also the mean power loss of the system over the process $\{X(t)|0 \leq t \leq T_{tot}\}$. This expression also involves a relationship between the phase of the response $X(t)$ and that of the signal $H_{ac}(t)$.

Figure 1 shows the normalized power loss $\langle P_{ac} \rangle / (h^2 \Omega)$ (the vertical axes) and associating quantities referred to in Sec. VI as functions of the noise intensity D (the horizontal axes). The circles in each upper panel of Figs. 1(a)–1(d) indicate the results obtained from the numerical simulation of Eq. (2.1) for each parameter of $K \in \{0, 0.1, 0.2, 0.3\}$ with $(\Omega, h) = (0.01, 0.01)$. The solid curves indicate analytical results for the power loss, the expression of which is given in Sec. VI. Hereafter, in all the results obtained from the numerical simulation, $\langle X \rangle$ denotes the statistical mean of a quantity X over 32 runs of Eq. (2.1) for $T_{tot} = 2048T$. The

numerical simulation of Eq. (2.1) was carried out with the second order stochastic Runge-Kutta method [38,39] with the time increment $T/2^{19}$. As shown in the upper panels of Figs. 1(a)–1(d), with K , the shape of $\langle P_{ac} \rangle$ changes from (a) a single peak shape ($K = 0$) to (b) that with plateau ($K = 0.1$), (c) that with two peaks and a local minimum ($K = 0.2$), and (d) that with a single peak and a local minimum ($K = 0.3$). When $\langle P_{ac} \rangle$ has two peaks and a local minimum, we call their left (right) peak the first (second) peak. The appearance of the local minimum in $\langle P_{ac} \rangle$ implies a change in dynamics induced by noise, the detail of which is discussed in Sec. VI. Typical time series of $X(t)$ around such characteristic points on $\langle P_{ac} \rangle$ are shown next.

Figure 2 shows the time series of $X(t)$ (solid curves) together with $H_{ac}(t)$ (waves of dotted curve) and $\text{sgn}[H_{ac}(t)]$ (rectangular waves of dashed lines): panels 2(a)–2(c) display those obtained at (a) $D = 0.016$, (b) 0.04, and (c) 0.082 near the three extrema on the curve for $K = 0.2$ in the upper panel of Fig. 1(c), and the panels 2(d)–2(f) display those obtained at (d) $D = 0.001$, (e) 0.041, and (f) 0.099 on the curve for $K = 0.3$ in the upper panel of Fig. 1(d). Here and hereafter, $\text{sgn}(x)$ denotes the sign function satisfying $\text{sgn}(x) = 1$ for $x \geq 0$, otherwise, -1 for $x < 0$.

In Fig. 2(a), we see the situation that the switching rate between the two states becomes comparable to Ω as the noise intensity reaches the first maximum. Here, the switching rate differs from the Kramers rate \tilde{w}_K , but includes an effect

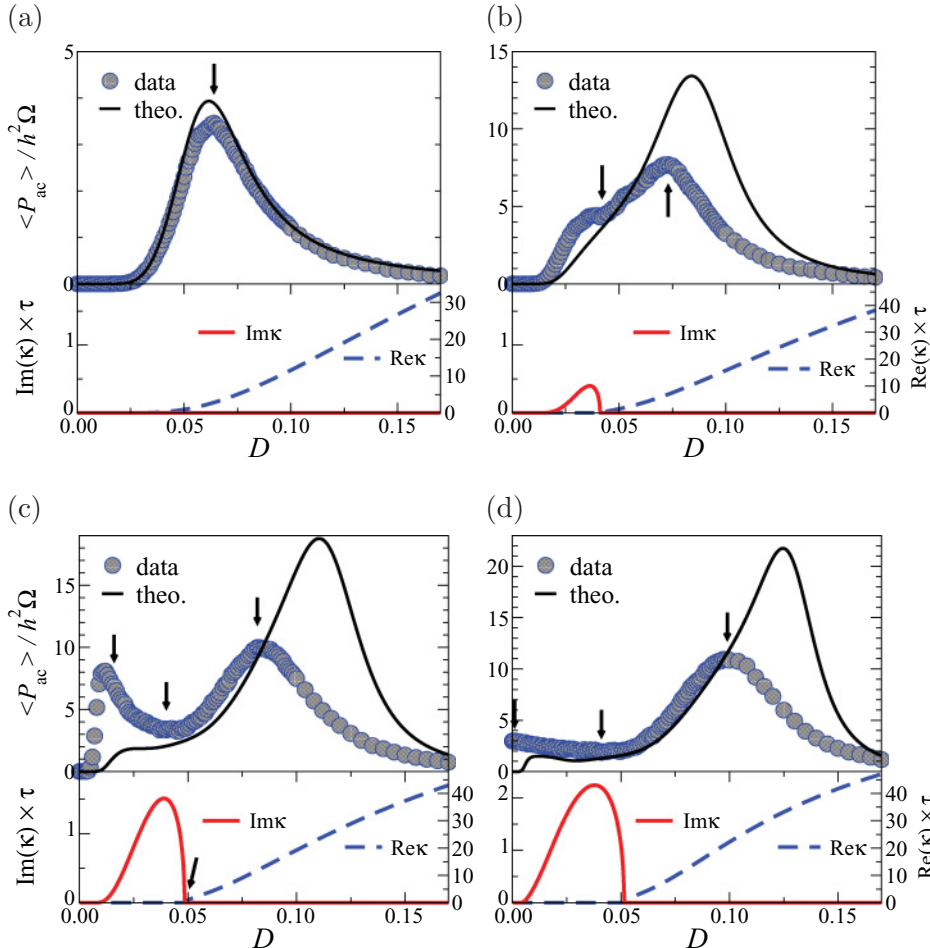


FIG. 1. (Color online) Normalized power loss $\langle P_{ac} \rangle / (h^2 \Omega)$ (upper parts of panels) and real and imaginary parts of κ (lower parts of panels) as functions of noise intensity D . In each upper part of the panels, the filled circles indicate the numerical results of $\langle P_{ac} \rangle / (h^2 \Omega)$ on D for each of the cases (a) $K = 0$, (b) 0.1, (c) 0.2, and (d) 0.3 with $(\Omega, h) = (0.01, 0.01)$. The solid curves represent the analytical result [Eq. (4.42)] based on the two-pole approximation in Sec. V. In each lower part of the panels, the solid (dashed) curve indicates the imaginary (real) part of κ (see Sec. V). The arrows indicate reference points for the data used in Figs. 2, 3, 5, and 6. The scales of the D axis are common for all the panels. The vertical scales are individual. The scales for the real (imaginary) part of κ are multiplied by τ , and are attached to the lower right (left) sides of the panels.

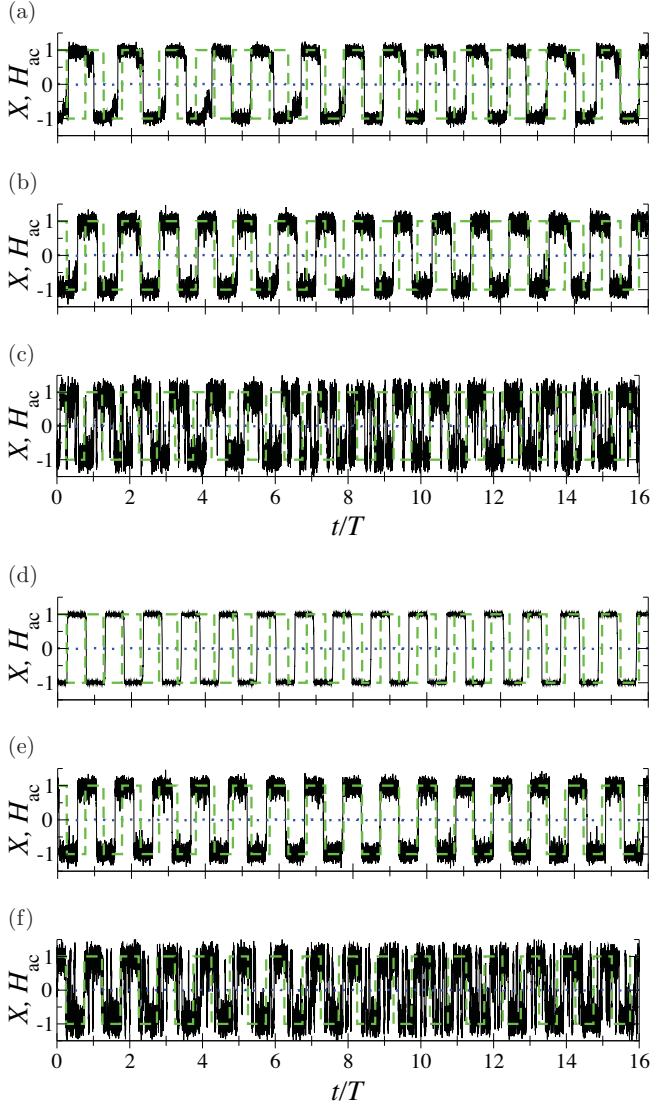


FIG. 2. (Color online) Time series of $X(t)$ (solid curves), $H_{ac}(t)$ (waves of dotted curve), and $\text{sgn}[H_{ac}(t)]$ (rectangular waves of dashed lines) obtained at (a) $D = 0.016$, (b) 0.042 , and (c) 0.084 near the three extrema on the curve for $K = 0.2$ in Fig. 1(c), and those obtained at (d) $D = 0.001$, (e) 0.041 , and (f) 0.099 on the curve for $K = 0.3$ in Fig. 1(d). The arrows in Figs. 1(c) and 1(d) indicate the observed points on D . The horizontal axis indicates the scaled time t/T .

of the TDFC, the analytic expression of which is given in Sec. IV. Such an effect appears in a sequence of the shifts in the first peaks of $\langle P_{ac} \rangle$ in the upper panels of Figs. 1(b)–1(d). This implies an enhancement in the switching rate due to the TDFC. As K increases beyond a certain value, the system undergoes a Hop bifurcation with a frequency of being less than Ω , which is intrinsic to the feedback loop. We see such an oscillation in Fig. 2(d).

In Figs. 2(b) and 2(e), we see that the relative phase between the rectangular wave and $X(t)$ slips, and that the mean frequency for the switching cycle of $X(t)$ is less than Ω . In Figs. 2(c) and 2(f), we can observe that the phase of $X(t)$ is approximately locked to that of $H_{ac}(t)$. This state is referred to as a phase-locked (PL) state. These results demonstrate

that the switching cycle becomes in concert with the external signal as the noise intensity reaches an appropriate level. This mechanism can be considered as a result of interplay between chattering behavior of the switching cycle and the TDFC. The chattering means an event of a multiple rapid switching (roundtrip) motion of $X(t)$ between the two states during one cycle of $H_{ac}(t)$ as can be seen in Figs. 2(c) and 2(f). As a result of chattering events, the mean frequency of the switching cycle will rise in a short term average over a few cycles of $H_{ac}(t)$. By mediating an appropriate frequency of the chattering events, the mean frequency of the switching cycles will be adapted to Ω , which is permitted under the TDFC. The PL state, therefore, can have a persistence against the phase slipping when the amplitude of the ac input is sufficiently large.

IV. DICHOTOMIC MODEL

The dichotomic model [5,6], which is obtained on the basis of the Kramers rate theory, is useful for a coarse-grained description of a bistable system. For that, the following situation is assumed: D is sufficiently smaller than the height of the potential barrier, i.e., $D \ll 1$, the amplitude of the ac input is sufficiently small ($h \ll 1$) (this enables one to assume a linear response relation from input to output) and the frequency Ω of the ac input is sufficiently small $\Omega \ll 1$ (this enables one to treat the external input as a quasistatic field).

In addition to these assumptions, we limit ourselves to the situation in which the delay time τ is not too long, and the feedback strength K is sufficiently small. As is mentioned in the context of the small time-delay approximation [18,27–29], if such parameters are out of the range, deviation of the effective potential in the Markovian approximation from its original one becomes large. Figure 3 shows such behaviors with the effective potential

$$V_{\text{eff}}(x) \equiv -\frac{D}{T_{\text{tot}}} \int_0^{T_{\text{tot}}} dt \log p(x, t) \quad (4.1)$$

at (a) $D = 0.064$, $K = 0$, (b) $D \in \{0.042, 0.073\}$, $K = 0.1$, (c) $D \in \{0.016, 0.042, 0.082\}$, $K = 0.2$, and (d) $D \in \{0.001, 0.041, 0.099\}$, $K = 0.3$ in $(\Omega, h) = (0.01, 0.01)$. We see that the shape of the effective potential considerably differs from the original one $V(x)$ in a small D regime, i.e., see the cases $D = 0.016$ and 0.001 in Figs. 3(c) and 3(d), and it appears with the region(s) of gradual slope or plateau as K increases. This tendency becomes large as τ increases. Thus, we limit the ranges of D , K , and τ to those in which a major deformation from $V(x)$ in the effective potential can be regarded to be $O(x^2)$. Since we have $\tau = \pi/\Omega$, the limitation for τ further limits the range of Ω . Let π/Ω_K be the upper limit of τ for a given D and K , then we have $\Omega_K < \Omega \ll 1$. The Ω_K may depend on a type of approximation.

In the situation mentioned above, the trajectory $X(t)$ fluctuates around either of the local minima of $V(X)$ almost all the time. The (C)PDF $p(x, t|\cdot)$ for the state $X(t) = x$ has sharp peaks around $x = \pm 1$, and it can quasistatically follow the external signal.

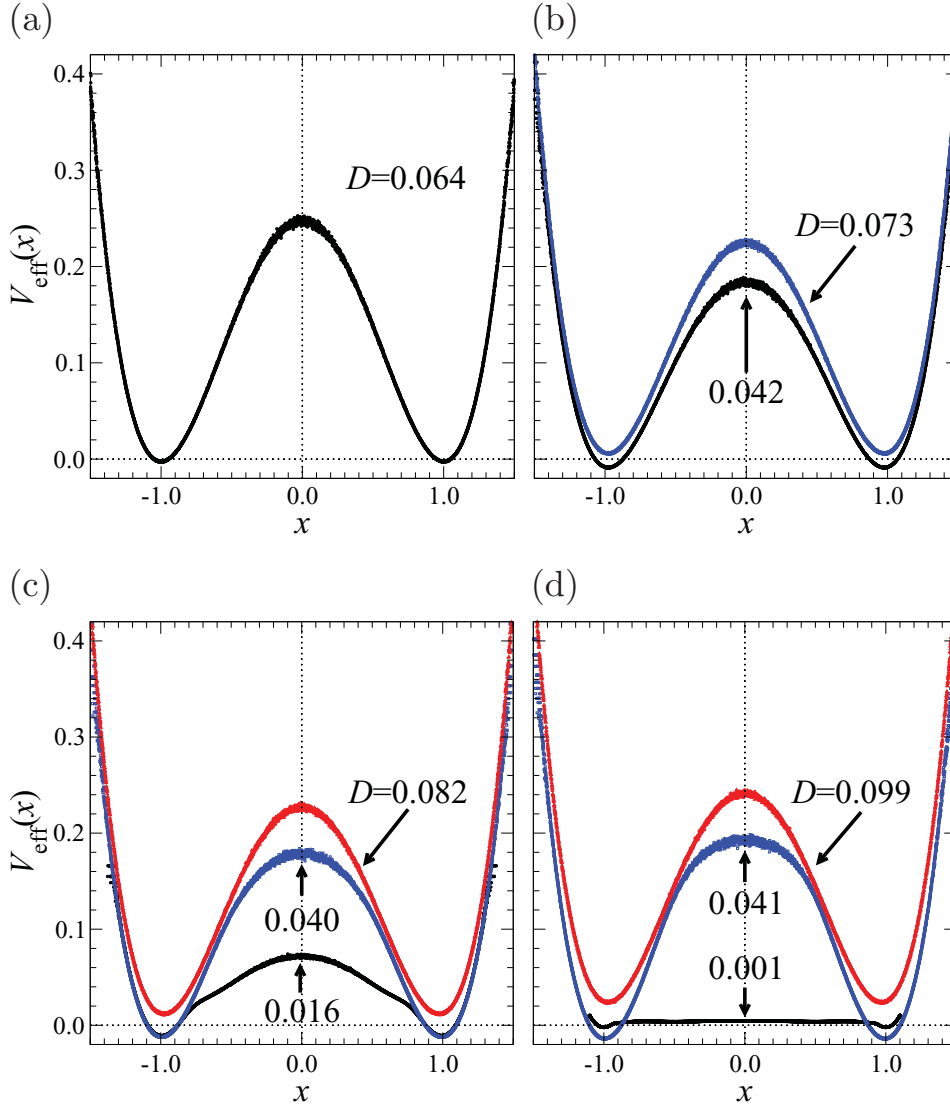


FIG. 3. (Color online) Effective potentials defined by Eq. (4.1) at (a) $D = 0.064$, $K = 0$, (b) $D \in \{0.042, 0.073\}$, $K = 0.1$, (c) $D \in \{0.016, 0.040, 0.082\}$, $K = 0.2$, and (d) $D \in \{0.001, 0.041, 0.099\}$, $K = 0.3$ with $(\Omega, h) = (0.01, 0.01)$. These positions on $\langle P_{ac} \rangle$ are indicated by the arrows in the upper panels of Fig. 1. The scales are all the same.

Assigning a dichotomous variable $\sigma \in \{-1, 1\}$ to $\text{sgn}[X(t)]$, probability for a state σ is defined as

$$P(\sigma, t|\cdot) \equiv \int_{-\infty}^{\infty} dx \Theta(\sigma x) p(x, t|\cdot). \quad (4.2)$$

As mentioned in Sec. II B, the “dot” indicates some condition if the probability is conditional, or else it indicates nothing. The master equation for the probabilistic process in the dichotomic model can be assumed as

$$\partial_t P(\sigma, t|\cdot) = W(\sigma, t|\cdot) P(-\sigma, t|\cdot) - W(-\sigma, t|\cdot) P(\sigma, t|\cdot), \quad (4.3)$$

with a transition rate $W(\sigma, t|\cdot)$ for a jump from a state $-\sigma$ to the other one σ .

All the estimation for $W(\sigma, t|\cdot)$ is described in Appendix A. Within the situation that a major deformation in the effective potential can be regarded as $O(x^2)$, we employ a piecewise linear hypothesis [Eq. (A5)] for the conditional average [Eq. (2.6)] [30]. By keeping the expression of $W(\sigma, t|\cdot)$ to be linear in h , the transition rate is obtained as

$$W(\sigma, t|\cdot) \approx \frac{1}{2} [w_A(t|\cdot) + \sigma \{w_h(t|\cdot) H_{ac}(t) - w_K(t|\cdot) B_1(t|\cdot)\}], \quad (4.4)$$

where, with $\bar{E} \equiv 1 - K A_1(t|\cdot)$,

$$w_A(t|\cdot) \equiv \frac{\sqrt{2}}{\pi} \bar{E} \exp\left(-\frac{\bar{E}^2}{4D}\right), \quad (4.5)$$

$w_K(t|\cdot) \equiv K(\bar{E}^2 - D)w_A(t|\cdot)/(2D\bar{E})$, $w_h(t|\cdot) \equiv \sqrt{\bar{E}}w_A(t|\cdot)/D$, and

$$A_1(t|\cdot) \equiv \sum_{\sigma} \frac{P(\sigma, t - \tau; \sigma, t|\cdot)}{P(\sigma, t|\cdot)}, \quad (4.6)$$

$$B_1(t|\cdot) \equiv \sum_{\sigma} \sigma \frac{P(\sigma, t - \tau; \sigma, t|\cdot)}{P(\sigma, t|\cdot)}. \quad (4.7)$$

Here, $\sum_{\sigma} \equiv \sum_{\sigma \in \{\pm 1\}}$, and $P(\sigma', t'; \sigma, t|\cdot)$ is the conditional joint probability for the states $\sigma' = \text{sgn}[X(t')]$ and $\sigma = \text{sgn}[X(t)]$. $B_1(t|\cdot)$ is assumed as a quantity of $O(h)$. Again, the transition rate depends on the conditional joint probability as in Eqs. (4.6) and (4.7), which inherits the condition(s) in Eq. (4.2). This expresses a nature of the non-Markovian process.

By substituting Eq. (4.4) into (4.3) without the condition “dot,” the master equation for the probability $P(\sigma, t)$ for the dichotomous states $\sigma \in \{\pm 1\}$ is obtained as

$$\partial_t P(\sigma, t) \approx W(\sigma, t)P(-\sigma, t) - W(-\sigma, t)P(\sigma, t) \quad (4.8)$$

$$\approx -w_A(t) \{P(\sigma, t) - 1/2\} + \sigma \{w_h H_{ac}(t) - w_K B_1(t)\} / 2, \quad (4.9)$$

where

$$A_1(t) = \sum_{\sigma} P(\sigma, t - \tau | \sigma, t), \quad (4.10)$$

$$B_1(t) = \sum_{\sigma} \sigma P(\sigma, t - \tau | \sigma, t). \quad (4.11)$$

Also, the master equation for the conditional probability $P(\sigma, t | \sigma', t')$ ($t > t'$) is obtained from Eqs. (4.3) and (4.4) as

$$\begin{aligned} \partial_t P(\sigma, t | \sigma', t') &\approx W(\sigma, t | \sigma', t') P(-\sigma, t | \sigma', t') \\ &\quad - W(-\sigma, t | \sigma', t') P(\sigma, t | \sigma', t') \quad (4.12) \\ &= -w_A(t | \cdot) \{P(\sigma, t | \cdot) - 1/2\} \\ &\quad + \sigma \{w_h(t | \cdot) H_{ac}(t) - w_K(t | \cdot) B_1(t | \cdot)\} / 2, \end{aligned} \quad (4.13)$$

where the dot abbreviates “ σ', t' .”

In Eq. (4.13), $w_A(t | \cdot)$ depends on the higher order conditional probability through the quantity $A_1(t | \cdot)$, which remains unknown so far. In order to reduce this complexity, this study attempts a delay-coordinate series expansion (DCSE), described in Appendix B, together with a Markov approximation. Instead of $P(\sigma, t | \sigma', t')$, let us use $Q(\sigma, t | \sigma', t') \equiv P(\sigma, t | \sigma', t') - 1/2$. The DCSE is a procedure for expanding $w_A(t | \cdot) Q(\sigma, t | \cdot)$ into a series of $Q(\sigma, t - k\tau | \cdot)$ on the delay coordinates with $k = 0, 1, 2, \dots$ and additional terms with the factor $B_1(t | \cdot)$. Appendix B estimates the DCSE up to the second order delay coordinate. Using this, Eq. (4.13) can be expanded as

$$\begin{aligned} \partial_t Q(\sigma, t | \sigma', t') &\approx - \sum_{k=0}^M w_k Q(\sigma, t - k\tau | \sigma', t') + \sigma w_B B_1(t) / 2 \\ &\quad + \sigma \{w_h(t) H_{ac}(t) - w_K(t) B_1(t)\} / 2, \end{aligned} \quad (4.14)$$

where M represents the order of the DCSE. The coefficients w_M , $w_K(t)$, $w_h(t)$, $w_B(t)$, and $B_1(t)$ depend on the condition “ σ', t' ” (“dot”). However, in the following treatment, we simplify Eq. (4.14) by replacing $A_1(t | \cdot)$ and $B_1(t | \cdot)$ involved in the coefficients with $A_1(t)$ and $B_1(t)$ in Eqs. (4.10) and (4.11). In these replacements, we assume $P(\sigma_\tau, t - \tau; \sigma, t | \cdot) / P(\sigma, t | \cdot) \approx P(\sigma_\tau, t - \tau | \sigma, t)$ in Eqs. (4.6) and (4.7). If the condition “ σ', t' ,” which is abbreviated by “dot,” satisfies $t - \tau \gg t'$, this assumption may be valid; however, we use the replacements even for $t - \tau < t' < t$ without justification hereafter. We call these replacements the Markov approximation.

Under the Markov approximation, for the case $M = 1$, the $w_k(t)$ ($k = 0, 1$) are given as

$$w_0 \equiv \frac{\sqrt{2}}{\pi} (1 - K) \exp \left\{ -\frac{(1 - K)^2}{4D} \right\} \quad [= w_A(t | \cdot) |_{A_1(t | \cdot) = 1}], \quad (4.15)$$

$$w_1 \equiv \frac{w_A(t) - w_0}{A_1(t) - 1}, \quad (4.16)$$

and $w_B = w_1$. Furthermore, for the case $M = 2$, w_0 , w_1 , w_2 , and w_B are given as Eq. (4.15), $w_1^{(2)}$ in Eq. (B7), $w_2^{(2)}$ in Eqs. (B13) and (B14), respectively. See Appendix B for details. This paper examines only the case $M = 1$.

A. Response function

$A_1(t)$ and $B_1(t)$ in Eq. (4.14) still remain unknown. This requires us to make a closed set of equations for them, and one must obtain backward and adjoint equations from Eq. (4.12). However, it is difficult to obtain them without the Markov approximation. This paper imposes the Markov approximation to construct the backward and the adjoint equations for a closed description, and its procedure is described in Appendix C.

First, let us consider the function $a(t, t') \equiv \sum_{\sigma} P(\sigma, t | \sigma, t') - 1$, which is concerned with $A_1(t)$ as $A_1(t) = 1 + a(t - \tau, t)$. From Eq. (4.13) or (4.14), the forward development of $a(t, t')$ ($t > t'$) obeys

$$\partial_t a(t, t') = -w_A(t) a(t, t') \approx - \sum_{j=0}^M w_j a(t - j\tau, t') \quad (t > t'). \quad (4.17)$$

The other required equations are made from the set of adjoint and backward master equations given in Eqs. (C4), (C6), and (C7) in Appendix C. From Eqs. (C10)–(C12), and the subsequent description, the associated adjoint and backward equations with $a(t, t')$ are obtained as

$$\partial_t a(t', t) \approx a(t', t) w_A(t) \quad (t' > t), \quad (4.18)$$

$$\partial_t a(t, t') \approx \sum_{j=0}^M w_j a(t - j\tau, t') \quad (t < t'), \quad (4.19)$$

$$\partial_t a(t', t) \approx - \sum_{j=0}^M a(t' - j\tau, t) w_j \quad (t' < t). \quad (4.20)$$

From Eqs. (4.19) and (4.20), making the differentiation of $a(t - \tau, t)$ with respect to t , we find $\partial_t a(t', t) |_{t'=t-\tau} + \partial_t a(t', t) |_{t'=t-\tau} = 0$. This indicates that $\dot{A}_1(t) = 0$ and $A_1(t)$ is a constant. Accordingly, all the coefficients in Eq. (4.14), i.e., $\{w_j(t)\}_{j=0}^M$, $w_h(t)$, etc., can be regarded as constants, then, hereafter, we omit the t dependence “(t)” from them. Also, the fact $\partial_t a(t', t) + \partial_t a(t', t) = 0$ from Eqs. (4.19) and (4.20) suggests that $a(t, t')$ has a translational invariance in time as $a(t, t') = \tilde{a}(t - t')$ for $t < t'$. For the case $t > t'$, from the second expression of Eqs. (4.17) and (4.18), we find $a(t, t') = \tilde{a}(t - t')$. However, the DCSE of Eq. (4.18), i.e., the counterpart to the third expression of Eq. (4.17), can not be exactly deduced because of the reason described below Eq. (C15) in Appendix C. Although this may be an obstacle

for the translational invariance $a(t, t') = \tilde{a}(t - t')$ for $t > t'$ in the form of the DCSE, hereafter, we assume that the relation $a(t, t') = \tilde{a}(t - t')$ approximately holds for both $t < t'$ and $t > t'$. Thus, by replacing $a(t, t')$ with $\tilde{a}(t - t')$ in Eqs. (4.17) and (4.19), we have

$$\partial_t \tilde{a}(t) \approx \begin{cases} -\sum_{j=0}^M w_j \tilde{a}(t - j\tau) & (t > 0), \\ \sum_{j=0}^M w_j \tilde{a}(t - j\tau) & (t < 0). \end{cases} \quad (4.21)$$

In addition to this, we impose the time-reversal symmetry $a(t, t') = a(t', t)$ [$\tilde{a}(-t) = \tilde{a}(t)$] as an assumption.

In a similar way, let us consider a function $B(t, t') \equiv \sum_{\sigma} \sigma P(\sigma, t | \sigma, t')$ [$= \sum_{\sigma} \sigma Q(\sigma, t | \sigma, t')$], which is concerned with $B_1(t)$ [$= B(t - \tau, t)$]. From Eq. (4.14) and the set of adjoint and backward master equations given in Eqs. (C4) and (C6)–(C9) in Appendix C, we obtain the forward and backward equations for $B(t, t')$ as follows:

$$\partial_t B(t, t') = -\sum_{j=0}^M w_j B(t - j\tau, t') + H'(t) \quad (t > t'), \quad (4.22)$$

$$\partial_t B(t', t) = -H_+(t) a(t', t) \quad (t' > t), \quad (4.23)$$

$$\partial_t B(t, t') = w_A B(t, t') + H_-(t) \quad (4.24)$$

$$= \sum_{j=0}^M w_j B(t - j\tau, t') + H_-(t) - w_B B_1(t) \quad (t < t'), \quad (4.25)$$

$$\partial_t B(t', t) = -H_-(t) a(t', t) \quad (t' < t), \quad (4.26)$$

where

$$H'(t) = w_h H_{ac}(t) - w_K B_1(t) + w_B B_1(t), \quad (4.27)$$

$$H_+(t) = w_h H_{ac}(t) - w_K B_1(t), \quad (4.28)$$

$$H_-(t) = -w_h H_{ac}(t) + w_K B_1(t) + 2\langle \dot{\sigma} \rangle_t. \quad (4.29)$$

The temporal evolution of $\langle \sigma \rangle_t \equiv \sum_{\sigma, \sigma_0} \sigma Q(\sigma, t | \sigma_0, t_0)$ $P(\sigma_0, t_0) [\approx \langle X(t) \rangle]$ is obtained from Eq. (4.14) as

$$\langle \dot{\sigma} \rangle_t \approx -\sum_{j=0}^M w_j(t) \langle \sigma \rangle_{t-j\tau} + H'(t), \quad (4.30)$$

where the initial condition $\langle \sigma \rangle_t = \langle \sigma \rangle_{t_0}$ at $t = t_0$ is imposed. Here, $H'(t)$ given in Eq. (4.27) represents an effective periodic force. A noticeable point is that Eq. (4.27) has the additional terms with the factor $B_1(t)$. The property that $B_1(t)$ has the same symmetry as $H_{ac}(t)$, i.e., $B_1(t) = -B_1(t - \tau)$ from Eq. (C3), implies that $B_1(t)$ has a close relationship to the phase entrainment of $X(t)$ to $H_{ac}(t)$ [30]. Section VIA gives details for that.

Also, from Eq. (4.14), an equation of development for the correlation function

$$C(t, t') = \sum_{\sigma, \sigma'} \sigma \sigma' Q(\sigma, t | \sigma', t') P(\sigma', t'), \quad C(t, t) = 1 \quad (4.31)$$

is derived as

$$\dot{C}(t, t') = -\sum_{j=0}^M w_j C(t - j\tau, t') + H'(t) \langle \sigma \rangle_{t'}. \quad (4.32)$$

Or, using $P(\sigma, t) = (1 + \sigma \langle \sigma \rangle_t)/2$, we have

$$C(t, t') = a(t, t') + \langle \sigma \rangle_{t'} B(t, t') \quad (t > t'). \quad (4.33)$$

The function $a(t, t')$ in Eqs. (4.17)–(4.20) has the same property as the response function in the context of the linear response theory [33]. In terms of $a(t, t')$, the solutions of Eqs. (4.22)–(4.26) and (4.30) can be expressed as

$$B(t, t') = \int_{t'}^t ds H_{\pm}(s) a(t, s), \quad (4.34)$$

$$\langle \sigma \rangle_t = a(t, t_0) \langle \sigma \rangle_{t_0} + \int_{t_0}^t ds H_+(s) a(t, s), \quad (4.35)$$

where, depending on the case $t > t'$ or $t < t'$, we have $H_+(t)$ or $H_-(t)$ in Eq. (4.34). Noting that

$$\begin{aligned} \int_{t'}^t ds H_{\pm}(s) \partial_t a(t, s) &= \mp w_A(t) B(t, t') \\ &= \mp \sum_{j=0}^M w_j B(t - j\tau, t') \pm w_B B_1(t), \end{aligned} \quad (4.36)$$

where the second line is derived from Eqs. (B12) and (C14), Eqs. (4.34) and (4.35) can be checked by their differentiation with respect to t . A distinctive point from the linear response relation in the conventional SR theory on the Markovian process is that $H_+(t)$ and $H_-(t)$ in Eqs. (4.34) and (4.35) include the term with $B_1(t)$ in addition to the external signal input $H_{ac}(t)$. A later consideration in Sec. VIA suggests that the factor $B_1(t)$ can be regarded as a measure for the effect of the coherent oscillation induced by noise and the TDFC.

B. Power loss

The power loss $\langle P_{ac} \rangle$ defined in Eq. (3.1) is related to the response function within the linear response theory [33]. The first term in the right-hand side of Eq. (4.35) vanishes in the limit $t_0 \rightarrow -\infty$. Therefore, supposing the asymptotic form of $\langle \sigma \rangle_t$ and $B_1(t)$ as $\langle \sigma \rangle_t \approx h \text{Re}[\tilde{\chi}(\Omega) e^{i\Omega t}]$ and $B_1(t) = h \text{Re}[\tilde{B}_1(\Omega) e^{i\Omega t}]$, respectively, the dynamic susceptibility $\tilde{\chi}(\omega)$ is estimated from Eqs. (4.28) and (4.35) as

$$\tilde{\chi}(\Omega) = \Xi(i\Omega) \{w_h - w_K \tilde{B}_1(\Omega)\}, \quad (4.37)$$

where $\Xi(\Gamma) = \int_0^\infty dt \tilde{a}(t) e^{-\Gamma t}$, and $\text{Re}[X]$ ($\text{Im}[X]$) denotes the real (imaginary) part of X . The Laplace transform of Eq. (4.21) reads as

$$\Xi(\Gamma) = \frac{\tilde{a}(0) - \sum_{j=1}^M w_j e^{-j\Gamma\tau} I_j(\Gamma)}{\Gamma + \sum_{j=0}^M w_j e^{-j\Gamma\tau}}, \quad (4.38)$$

where $I_j(\Gamma) \equiv \int_0^{j\tau} \tilde{a}(t) e^{-\Gamma t} dt$ ($j = 1, 2, \dots$). Also, from Eqs. (4.29) and (4.34), for $B_1(t) = B(t - \tau, t)$, we have

$$\tilde{B}_1(\Omega) = I_1(i\Omega) \{-w_h + w_K \tilde{B}_1(\Omega) + 2i\Omega \tilde{\chi}(\Omega)\}. \quad (4.39)$$

Then, we rewrite Eqs. (4.37) and (4.39) as

$$\hat{G}(\Omega) \begin{pmatrix} \tilde{\chi}(\Omega) \\ \tilde{B}_1(\Omega) \end{pmatrix} = w_h \begin{pmatrix} 1 - \sum_{j=1}^M (-1)^j w_j I_j(i\Omega) \\ -I_1(i\Omega) \end{pmatrix}, \quad (4.40)$$

with the matrix

$$\hat{G}(\Omega) \equiv \begin{pmatrix} i\Omega + \sum_{j=0}^M (-1)^j w_j w_K \{1 - \sum_{j=1}^M (-1)^j w_j I_j(i\Omega)\} \\ -2i\Omega I_1(i\Omega) & 1 - w_K I_1(i\Omega) \end{pmatrix}. \quad (4.41)$$

From Eq. (4.40), we can obtain $\tilde{\chi}(\Omega)$ and $\tilde{B}(\Omega)$. In terms of $\tilde{\chi}(\Omega)$, the power loss is expressed as

$$\langle P_{ac} \rangle \approx -\frac{h^2 \Omega}{2} \text{Im} [\tilde{\chi}(\Omega)]. \quad (4.42)$$

Here, the valid ranges of Ω , K , and D must be restricted to those in which the determinant of the matrix (4.41) is not too small or does not vanish. This limitation corresponds to that for the permissible deformation of the effective potential (4.1) under consideration. Similar circumstances also appear in the analysis based on the small time-delay approximation [27,28].

V. TWO-POLE EXPANSION

Let us consider the fundamental solution for $\tilde{a}(t)$ ($t \geq 0$) in Eq. (4.21) for the case $M = 1$, i.e.,

$$\partial_t \tilde{a}(t) = -w_0 \tilde{a}(t) - w_1 \tilde{a}(t - \tau). \quad (5.1)$$

The same equation is treated in Refs. [12,40]. First, we find a solution of Eq. (5.1) for $|t| \leq \tau$ with the boundary condition $\tilde{a}(t) = \tilde{a}(-t)$. The transformation $I_1(\Gamma) = \int_0^\tau \tilde{a}(t) e^{\Gamma t} dt$ rewrites Eq. (5.1) as

$$(w_0 - \Gamma) I_1(\Gamma) + w_1 e^{\Gamma \tau} I_1(-\Gamma) = \tilde{a}(0) - \tilde{a}(\tau) e^{\Gamma \tau}. \quad (5.2)$$

By using this, we obtain

$$\int_{-\tau}^\tau \tilde{a}(t) e^{\Gamma t} dt = I_1(\Gamma) + I_1(-\Gamma) = \tilde{C}_0(\Gamma) \tilde{a}(0) + \tilde{C}_1(\Gamma) \tilde{a}(\tau), \quad (5.3)$$

where

$$\tilde{C}_0(\Gamma) \equiv \frac{2}{\kappa^2 - \Gamma^2} \{w_0 - w_1 \cosh(\Gamma \tau)\}, \quad (5.4)$$

$$\tilde{C}_1(\Gamma) \equiv \frac{2}{\kappa^2 - \Gamma^2} \{w_1 - w_0 \cosh(\Gamma \tau) - \Gamma \sinh(\Gamma \tau)\}, \quad (5.5)$$

and $\kappa \equiv \sqrt{w_0^2 - w_1^2}$. In this paper, the integral transformation in the left-hand side of Eq. (5.3) is referred to as the finite Laplace transform. Since the functions $\{\tilde{C}_j(\Gamma)\}_{j=0,1}$ have two poles $\Gamma = \kappa$ and $-\kappa$ on the complex plane, we call this analysis two-pole expansion (approximation). In this way, the analysis based on the M th order DCSE is called $2M$ -pole expansion. The poles $\pm\kappa$ lie on either the real or pure imaginary axis, depending on D .

The inverse transformation of Eq. (5.3) yields

$$\tilde{a}(t) = C_0(t) \tilde{a}(0) + C_1(t) \tilde{a}(\tau), \quad (5.6)$$

where $C_j(t) \equiv (2\pi i)^{-1} \int_{-i\infty}^{i\infty} d\Gamma \tilde{C}_j(\Gamma) e^{-\Gamma t}$ ($j = 0, 1$), i.e.,

$$C_0(t) = -\frac{w_0}{\kappa} S_x(\kappa, t) + \frac{w_1}{\kappa} S_x(\kappa, \tau) \cosh(\kappa t), \quad (5.7)$$

$$C_1(t) = -\frac{w_1}{\kappa} S_x(\kappa, t) + \frac{w_0}{\kappa} S_x(\kappa, \tau) \cosh(\kappa t) + C_x(\kappa, \tau) \cosh(\kappa t). \quad (5.8)$$

Here, the functions $S_x(\kappa, t)$ and $C_x(\kappa, t)$ are defined as

$$S_x(\kappa, t) \equiv e^{\kappa t} \Theta(-\text{Re}\kappa) - e^{-\kappa t} \Theta(\text{Re}\kappa), \quad (5.9)$$

$$C_x(\kappa, t) \equiv e^{\kappa t} \Theta(-\text{Re}\kappa) + e^{-\kappa t} \Theta(\text{Re}\kappa), \quad (5.10)$$

with $\Theta(\dots)$ being the Heaviside's unit step function: $\Theta(x) = 1$ for $x > 0$, $\Theta(x) = 0$ for $x < 0$, and $\Theta(x) = 1/2$ for $x = 0$, e.g., in Eq. (5.10), $C_x(\kappa, t) = e^{-\kappa t}$ for a positive real κ or $C_x(\kappa, t) = \cosh(\kappa t)$ for a pure imaginary κ .

The boundary condition at $t = \tau$ in Eq. (5.6) leads to

$$\tilde{a}(\tau) = \frac{w_0 - w_1 \cosh(\kappa \tau)}{-w_1 + w_0 \cosh(\kappa \tau) + \kappa \sinh(\kappa \tau)}, \quad (5.11)$$

where we set $\tilde{a}(0) = 1$. With the expression of $\tilde{a}(\tau)$ in Eq. (5.11), a self-consistent equation for A_1 is given as

$$A_1 = 1 + \tilde{a}(\tau). \quad (5.12)$$

For given parameters D , Ω , and K , A_1 is determined by numerically solving Eq. (5.12) together with Eqs. (4.5), (4.15), and (4.16).

Furthermore, let us define $\Delta_n(\Gamma) \equiv \int_{(n-1)\tau}^{\tau} \tilde{a}(t) e^{\Gamma t} dt$ ($n > 1$). From Eq. (5.1), $\Delta_n(\Gamma)$ satisfies

$$(w_0 - \Gamma) \Delta_n(\Gamma) + w_1 e^{\Gamma \tau} \Delta_{n-1}(\Gamma) = \tilde{a}_{n-1} e^{(n-1)\Gamma \tau} - \tilde{a}_n e^{n\Gamma \tau}, \quad (5.13)$$

where $\tilde{a}_n \equiv \tilde{a}(n\tau)$. Therefore, via the inverse transformation $(2\pi i)^{-1} \int_{-i\infty}^{i\infty} \Delta_n(\Gamma) e^{-\Gamma t} d\Gamma$ ($n > 1$), we obtain

$$\begin{aligned} \tilde{a}[(n-1)\tau + u] &= \tilde{a}_{n-1} e^{-w_0 u} \\ &\quad - w_1 \int_0^u ds e^{-w_0(u-s)} \tilde{a}[(n-2)\tau + s] \end{aligned} \quad (5.14)$$

for $0 < u < \tau$ [$t \equiv (n-1)\tau + u$]. Using Eqs. (5.6) and (5.14), we can find $\tilde{a}(n\tau + u)$ ($0 \leq u < \tau$) for $n > 0$ [12,40].

VI. NUMERICAL RESULTS AND DISCUSSION

In this section, we examine the results of the analysis. Sections VIA, VIB, and VIC deal with the power loss, correlation function, and the power spectral density, respectively.

A. Power loss

The analytical result for the power loss $\langle P_{ac} \rangle$ based on the two-pole expansion is given by Eq. (4.42) with the dynamic susceptibility $\tilde{\chi}(\Omega)$ in Eqs. (4.40) and (4.41) for $M = 1$. In the actual calculation of $\langle P_{ac} \rangle$, at first, A_1 and $\{w_j\}_{j=0,1}$ are determined by solving Eq. (5.12) with Eqs. (4.15), (4.16), and (5.11) for a given set of parameters, i.e., D , Ω , and K . Then, the obtained values are substituted into the associated equations with $\langle P_{ac} \rangle$. In the present cases, we have $0.001 < \Omega_K < 0.01$. The upper panels of Figs. 1(a)–1(d) in Sec. III show the analytical results for $\langle P_{ac} \rangle$ versus D with solid curves, together with the results obtained from the numerical simulation of Eq. (2.1) with circles, for the cases (a) $K = 0$, (b) 0.1,

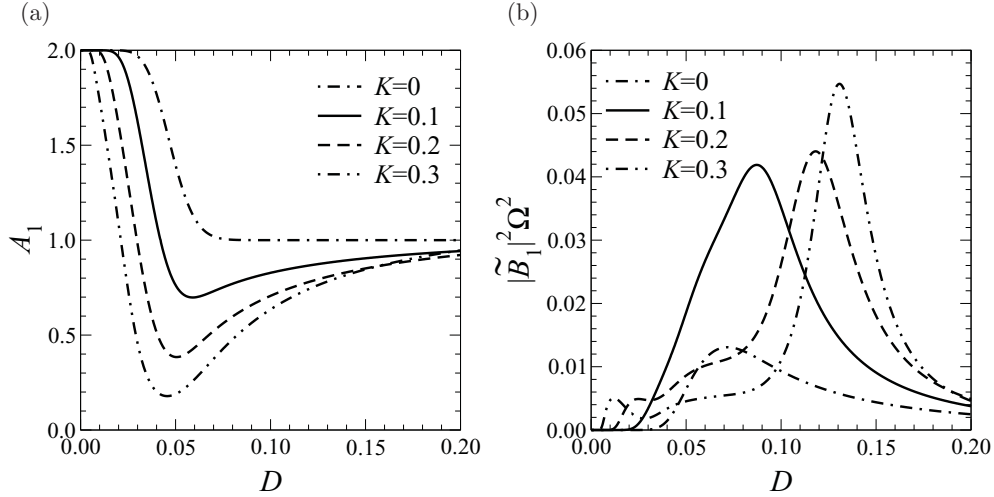


FIG. 4. (a) A_1 and (b) $|\tilde{B}_1|^2 \Omega^2$ as functions of D . They are obtained from Eqs. (5.12) and (4.40), respectively, on the basis of the two-pole approximation ($M = 1$). The curves in both panels correspond to the results for $K = 0$ (dashed-dotted curves), 0.1 (solid curves), 0.2 (dashed curves), and 0.3 (dashed-double-dotted curves) with $(\Omega, h) = (0.01, 0.01)$.

(c) 0.2, (d) 0.3 with $(\Omega, h) = (0.01, 0.01)$. Except for the case $K = 0$, the analytical results do not precisely agree with the simulation results in their small D regimes. On the other hand, one can see that their qualitative shapes in both results have similarities in their large D regimes. Namely, the region of the middle-right slope and the plateau of the solid curves in Figs. 1(c) and 1(d) roughly agree with that of the simulation results. The deviation in the small D regions reflects the large deformation of the effective potential equation (4.1) as shown in Fig. 3. Observing the shapes of the potential in Fig. 3 and the corresponding regions of D in Fig. 1, we can admit that the piecewise linear approximation qualitatively works in the range beyond the minimal point in D of $\langle P_{ac} \rangle$.

Some studies consider that the bimodal peak structure in $\langle P_{ac} \rangle$ is a superposition of two kinds of peaks, one is due to the original SR mechanism and the other one comes from the CR-like effect due to the TDFC [20,21,30]. Although $\langle P_{ac} \rangle$ in the present analysis does not clearly reveal the bimodal peak structure in Fig. 1(c), we can specify each of the bimodal peaks with other quantities. Figure 4 shows (a) A_1 and (b) $|\tilde{B}_1|^2$ as functions of D . The quantities A_1 and $|\tilde{B}_1|^2$ are obtained from Eqs. (4.15), (4.16), (4.40), (4.41), (5.11), and (5.12). We see that, in Fig. 4(a), the region in which A_1 steeply decreases in D shifts its position in D to the left as K increases; on the other hand, in Fig. 4(b), the peak of $|\tilde{B}_1|^2$ shifts its position to the right. From Fig. 4(a) and $\langle P_{ac} \rangle$ in the upper panels of Figs. 1(a)–1(d), we can notice that the steeply decreasing region of A_1 corresponds to the first peak of $\langle P_{ac} \rangle$. This can be relevant to the exponential dependence of w_A (or w_h) on A_1 in Eq. (4.5). Namely, in the region where A_1 steeply changes, w_A correspondingly changes, and the region can have a resonance point on D , which satisfies $w_A \approx \Omega$. This is similar to the conventional SR. Likewise, from the observation of Fig. 4(b) and $\langle P_{ac} \rangle$ in the upper panels of Figs. 1(a)–1(d), we find that the peak point of $|\tilde{B}_1|^2$ on the D axis corresponds to the second peak point of $\langle P_{ac} \rangle$. As mentioned after Eqs. (4.30) and (4.36), $|\tilde{B}_1|^2$ can be regarded as a measure for the phase entrainment to $H_{ac}(t)$. This can be concluded by the numerical evidence that

the maximum point of $\langle P_{ac} \rangle$ in $K > 0$ corresponds to the PL state [Figs. 2(c) and 2(f)]. In this way, the two quantities A_1 and $|\tilde{B}_1|^2$ can qualitatively specify the first and the second peaks of $\langle P_{ac} \rangle$. Although $\langle P_{ac} \rangle$ includes these quantities, a roughness of approximation, e.g., the piecewise linear hypothesis equation (A5), may destruct the bimodal peak structure.

We also show the D dependence of the pole κ defined in Eqs. (5.4) and (5.5) in the lower panels of Figs. 1(a)–1(d). We see that κ is pure imaginary below a certain value of D in the cases $K > 0$; on the other hand, as D increases, through the degenerate point at which the two poles $\pm\kappa$ merge at the origin on the complex plane, κ becomes real and increases. It is also found the minimal point or plateau of $\langle P_{ac} \rangle$ corresponds to the degenerate point ($\kappa = 0$). Thus, we can expect that the minimal point of $\langle P_{ac} \rangle$ indicates a sort of critical point in dynamics. The next section shows the change of behavior in the correlation function depending on D .

B. Correlation function

In the correlation function (4.33), the first term is given by $\tilde{a}(t - t')$ with Eqs. (5.6)–(5.12), and (5.14). $\langle \sigma \rangle_t$ and $B(t, t')$ of the second term are given by the asymptotic form of Eq. (4.35) in $t_0 \rightarrow -\infty$, and Eq. (4.34) for the case $t > t'$, respectively. Putting $H_+(t) = h \text{Re}[\tilde{H}_+ e^{i\Omega t}]$ in Eqs. (4.34) and (4.35), $\langle \sigma \rangle_t$ and $B(t, t')$ are estimated as

$$\langle \sigma \rangle_t \approx h \text{Re}[e^{i\Omega t} \tilde{H}_+ \Xi(i\Omega)], \quad (6.1)$$

$$B(t, t') = h \text{Re} \left[e^{i\Omega t} \tilde{H}_+ \int_0^{t-t'} ds e^{-i\Omega s} \tilde{a}(s) \right]. \quad (6.2)$$

By applying the averaging procedure $C(t) \equiv \int_{T_0}^{T_0+T} C(s + t, s) ds / T$ ($T_0 \rightarrow \infty$) to Eq. (4.33) after substituting Eqs. (6.1) and (6.2) into Eq. (4.33), we obtain

$$C(t) = \tilde{a}(t) + \frac{h^2}{2} |\tilde{\chi}(\Omega)|^2 \text{Re} \left[\frac{e^{i\Omega t}}{\Xi(i\Omega)} \int_0^t ds e^{-i\Omega s} \tilde{a}(s) \right], \quad (6.3)$$

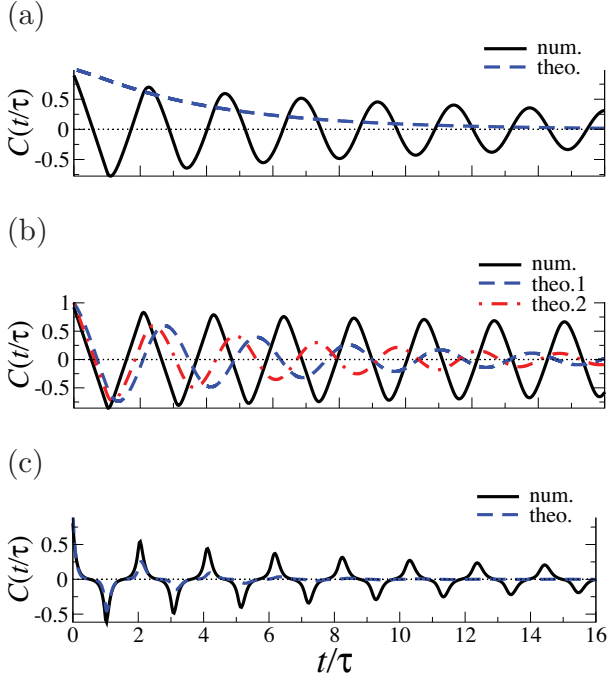


FIG. 5. (Color online) The correlation functions at the three extrema of $\langle P_{ac} \rangle$ in Fig. 1(c) ($K = 0.2$). The solid and dashed curves in the panels show the scaled correlation functions $C(t/\tau)$ obtained from the numerical simulation of Eq. (2.1) (solid curves) and the analytical results of Eq. (6.3) at (a) $D = 0.016$, (b) 0.04, and (c) 0.082, with positions on the curve $\langle P_{ac} \rangle$ versus D indicated by the arrows in the upper panel of Fig. 1(c). The horizontal axes are scaled as t/τ . The dashed-dotted curve in panel (b) indicates the analytical result of Eq. (6.3) at $D \approx 0.0484$ (the vanishing point of κ), the position of which is indicated by the arrow in the lower panel of Fig. 1(c). In these curves, the oscillation component composed of the harmonics of Ω is eliminated.

where $\tilde{\chi}(\Omega) = \Xi(i\Omega)\tilde{H}_+$ from Eq. (4.37). In the limit $t \rightarrow \infty$, the last term becomes $h^2 |\tilde{\chi}(\Omega)|^2 \cos(\Omega t)/2$.

Figure 5 shows the correlation functions obtained from the numerical simulation of Eq. (2.1) (solid curves) and the analytical results (dashed curves) at (a) $D = 0.016$, (b) 0.04, and (c) 0.082 in $(K, h, \Omega) = (0.2, 0.01, 0.01)$, where these positions on the curve $\langle P_{ac} \rangle$ versus D are indicated by the arrows in the upper panel of Fig. 1(c). The solid curves are made by the Fourier transform of the power spectral density from the time series $\{X(t)|0 \leq t \leq T_{\text{tot}}\}$, but the line spectrums at the harmonics of Ω are eliminated (see Fig. 6). The dashed curves represent the first term of Eq. (6.3), i.e., $\tilde{a}(t)$, where t is replaced with t/τ . The dashed-dotted curve in Fig. 5(b) represents the first term of Eq. (6.3) at $D \approx 0.0484$, which corresponds to the vanishing point of the pole κ [Fig. 1(c)], and gives a reference point comparable to the minimal point of $\langle P_{ac} \rangle$ in the simulation result. We see that the solid and dashed curves in Fig. 5(a) quite differ. This disagreement comes from the roughness of the piecewise linear approximation. Figure 5(b) shows that, in two comparisons with the dashed and the dashed-dotted curves to the solid one, the dashed-dotted curve is closer to the solid one, while its frequency is still slightly different. For more quantitative agreement, it is necessary to improve the employed approximations. The

solid curve in Fig. 5(b) exhibits a characteristic behavior of the correlation function that the relaxation time of the oscillation grows near the minimal point of $\langle P_{ac} \rangle$. This is consistent with the observation that the vanishing point of the pole κ corresponds to the minimal point, and that $|\kappa|$ is the inverse of a characteristic time scale of the correlation function. Figure 5(c) shows the correlation function at the second peak of $\langle P_{ac} \rangle$. One can see that the modulation frequency of the analytical result agrees with that of the simulation result.

C. Power spectral density

Power spectral density is obtained through the Fourier transform of the correlation function, i.e., $S(\omega) \equiv 2\text{Re} \int_0^\infty dt e^{-i\omega t} C(t)$. From Eq. (6.3), we have

$$S(\omega) = S_n(\omega) + \frac{\pi h^2}{2} |\tilde{\chi}(\Omega)|^2 \{\delta(\Omega - \omega) + \delta(\Omega + \omega)\}, \quad (6.4)$$

$$S_n(\omega) = 2\text{Re} \Xi(i\omega) + \frac{h^2}{2} |\tilde{\chi}(\Omega)|^2 \text{Im} \left[\frac{\Xi(i\omega)}{\Xi(i\Omega)} \frac{1}{\omega - \Omega} + \frac{\Xi(i\omega)}{\Xi(-i\Omega)} \frac{1}{\omega + \Omega} \right]. \quad (6.5)$$

Figure 6 shows the power spectral densities obtained from the numerical simulation of Eq. (2.1) (circles) and the analytical results (dashed curves) at (a) $D = 0.016$, (b) 0.04, and (c) 0.082 in $(K, h, \Omega) = (0.2, 0.01, 0.01)$. The dashed curves indicate the first term in the right-hand side of Eq. (6.5), i.e., we drop the terms associated with the ac input signal. The dashed-dotted curve in Fig. 6(b) indicates the analytical result at $D \approx 0.0484$ (the vanishing point of κ). As mentioned in Sec. VI B, this point of D is related to the minimal point of $\langle P_{ac} \rangle$ in the simulation results. In the same way as Fig. 5(a), in Fig. 6(a), the analytical result quite differs from the simulation result. In Fig. 6(b), both the peak position in ω and the magnitude of the analytical curve deviate from the simulation result. However, we see that the dashed-dotted curves are closer to the solid curves than the dashed curves. This tendency implies that we can adjust the analytical result by more careful approximation than Eq. (A5). In Fig. 6(c), we see that the peak positions of the two curves almost agree. Figures 6(b) and 6(c) demonstrate that, as D increases, the peak position of $S_n(\omega)$ in ω reaches the position of the line spectrum at $\omega = \Omega$, and the signal-to-noise ratio, i.e., $h^2 |\tilde{\chi}(\Omega)|^2 / S_n(\Omega)$, improves. This manifests the frequency adaptation caused by the interplay of noise and the TDFC.

VII. SUMMARY

This paper investigated the property of controlled stochastic resonance (SR) in a bistable system under the time-delayed feedback control. As an extension to the dichotomic Markov approximation in Refs. [12,30], a systematic approach, the DCSE and the associating Markov approximation, for obtaining the response function was proposed. As a primitive implementation, the analysis based on the two-pole expansion was reported. In this approach, first we obtain the master equation for the dichotomous states, i.e., Eq. (4.3). This step needs a hypothetical treatment for the conditional average Eq. (2.6). This paper employed the piecewise linear hypothesis

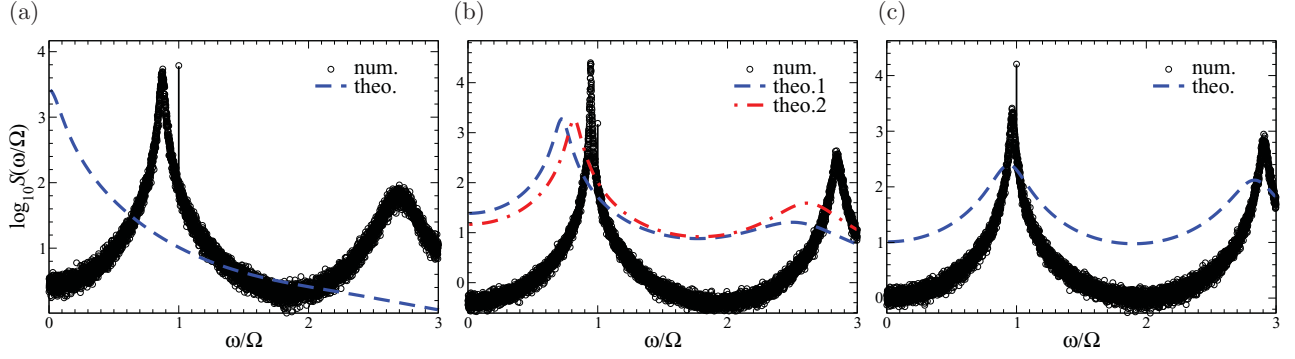


FIG. 6. (Color online) The power spectral densities at the three extrema of $\langle P_{ac} \rangle$. The circles and dashed curves in the panels show the results obtained from the numerical simulation of Eq. (2.1) (circles) and the analytical results of Eqs. (6.4) and (6.5) (dashed curves) at (a) $D = 0.016$, (b) 0.04 , and (c) 0.082 , with positions on $\langle P_{ac} \rangle$ indicated by the arrows in the upper panel of Fig. 1(c). The dashed-dotted curve in panel (b) indicates the analytical result of Eqs. (6.4) and (6.5) at $D \approx 0.0484$ (the vanishing point of κ), the position of which is indicated by the arrow in the lower panel of Fig. 1(c). In the analytical curves, the first term of Eq. (6.5) is plotted. The horizontal axes are scaled as ω/Ω . The vertical axes indicate $\log_{10} S(\omega/\Omega)$. The line at $\omega/\Omega = 1$ in each panel indicates the spectrum intensity of the external signal.

(A5) for it. Second, the master equation is expanded into the series on the delay coordinate system, i.e., Eq. (4.14). Third, a set of closed equations associated with the response function, i.e., Eqs. (4.17)–(4.20) and (4.22)–(4.29), is obtained. In this paper, this step employed the Markov approximation and utilized the symmetric property of the system to obtain the backward and adjoint master equations. Finally, the finite pole approximation for the response function is carried out. Then, we can evaluate the power loss, the correlation function, and the power spectral density.

A remarkable result obtained through the DCSE is the linear response relation (4.35), where in Eqs. (4.28) and (4.29) the additional term with $B_1(t)$ manifests the coherent oscillation induced by the TDFC. As shown in Fig. 4, the quantity $B_1(t)$ together with A_1 well characterizes the bimodal peak structure. Generally, linear response relation provides a fundamental property of SR. While systematic approach for linear response relation is firmly formulated in Markovian systems, it is nontrivial in non-Markovian systems because of the hierarchical dependence of conditional probabilities. For this problem concerning SR, the treatments up to date have been insufficient to self-consistently incorporate the non-Markovian property, and have not derived the relation as mentioned above. The present approach proposes a method to convert and approximate the non-Markovian transition probability flux to the series of memory flux on the delay-coordinate system. This is the first step for a systematic and self-consistent determination of the effective potential, which has been assumed with the piecewise linear hypothesis, by extracting an essence of the non-Markovian dynamics.

It was shown that the D -dependent behavior of the pole well characterizes the change in dynamics as D changes, where the degenerate point of poles corresponds to the minimal point of the power loss on D . The comparisons between the analytical and the simulation results for the quantities mentioned above showed that, in the region of D beyond the minimal point of the power loss, the analytical results qualitatively reveal the simulation results; on the other hand, below the minimal point on D , the analytical results drop their quality. The latter circumstances come from the deformation of the effective

potential. For a more quantitative estimation, more precise approximations, in particular, a more extended treatment of the piecewise linear hypothesis (A5), will be required. The future plans of this study are to improve the employed approximations and to examine more higher order pole expansion, and also to extend the method to systems with the asymmetric bistable potential.

APPENDIX A: KRAMERS RATE

In addition to the assumptions mentioned in the beginning of Sec. IV, we assume that, after passing a sufficiently long-term development, a CPDF $p(x, t | \cdot, \{x\}_i)$ [a CJPDF $p(x, t; x_\tau, t - \tau | \cdot, \{x\}_i)$] converges on a certain asymptotic CPDF $p(x, t | \cdot)$ [CJPDF $p(x, t; x_\tau, t - \tau | \cdot)$], independent of the initial process $\{x\}_i$.

Under the assumptions, the CPDF $p(x, t | \cdot)$ for the state $X(t) = x$ has sharp peaks around the two points $x = -1$ and 1 , and it almost vanishes around the origin. Let us define three subdomains for x of $p(x, t | \cdot)$ as $\mathbb{D}_- \equiv \{x | -\infty < x \leq x_-\}$, $\mathbb{D}_+ \equiv \{x | x_+ \leq x < \infty\}$, and $\mathbb{D}_0 \equiv \{x | x_- < x < x_+\}$ [41]. Here, x_+ and x_- are constants satisfying $-1 < x_- < 0$ and $0 < x_+ < 1$. Let us assume $x_- = -x_+$ by virtue of symmetry. As mentioned above, the CPDF almost vanishes on the domain \mathbb{D}_0 , and we assume $p(\pm 1, t | \cdot) \gg p(x_\pm, t | \cdot)$.

In the framework of the dichotomic model [5,6], the probability flux \mathcal{J} in Eq. (2.4) can be read as $\mathcal{J} \approx 0$ for \mathbb{D}_\pm and $\mathcal{J} \approx J_t$ for \mathbb{D}_0 , where J_t is a time-dependent probability current without dependence on x . Then, from Eqs. (2.4)–(2.6), for each domain of $x \in \mathbb{D}_-$ and $x \in \mathbb{D}_+$, the CPDF $p(x, t | \cdot)$ satisfies $p(x, t | \cdot) = p(x_\pm, t | \cdot) e^{-\Phi(x, x_\pm)}$, where the function $\Phi(x, x_*)$ is defined as

$$\Phi(x, x_*) \equiv \frac{1}{D} \int_x^{x_*} dy [-V'(y) + H_{ac}(t) - K \{y + \langle x_\tau | y, t; \cdot \rangle\}]. \quad (\text{A1})$$

Using this, the conditional probability $P(\sigma, t | \cdot)$ defined in Eq. (4.2) for the dichotomic observable

$\sigma = \text{sgn}[X(t)] \in \{-1, 1\}$ can be approximately expressed as

$$P(\sigma, t|\cdot) \approx \int_{x \in \mathbb{D}_\sigma} dx e^{-\Phi(x, x_\sigma)} p(x_\sigma, t|\cdot), \quad (\text{A2})$$

where σ 's in x_σ and \mathbb{D}_σ indicate the sign “+” or “−” corresponding to +1 or −1. For $x \in \mathbb{D}_0$, by multiplying the second line of Eq. (2.4) by $e^{\Phi(x, 0)}$ and integrating it from x_- to x_+ , we obtain

$$-D e^{\Phi(x, 0)} p(x, t|\cdot) \Big|_{x_-}^{x_+} = J_t \int_{x_-}^{x_+} dx e^{\Phi(x, 0)}. \quad (\text{A3})$$

The temporal development of $P(\sigma, t|\cdot)$ is given by $\dot{P}(\sigma, t|\cdot) \approx \sigma J_t$. By combining this with Eqs. (A3) and (A2), we obtain the master equation (4.3) for the probabilistic process between the dichotomous states with the transition rate (the so-called Kramers rate) $W(\sigma, t|\cdot)$ as

$$W(\sigma, t|\cdot) \equiv D \left[\int_{x \in \mathbb{D}_{-\sigma}} dx e^{U(x)} \int_{x_-}^{x_+} dy e^{-U(y)} \right]^{-1}, \quad (\text{A4})$$

where $U(x) \equiv -\Phi(x, 0)$. The “dot” in $W(\sigma, t|\cdot)$ stands for the condition that corresponds to that of $P(\sigma, t|\cdot)$ if it is conditional.

Through the conditional average $\langle x_\tau | x, t; \cdot \rangle$, the force [Eq. (2.5)] or “potential” function [Eq. (A1)] depends on the path of the state before t . Here, by the piecewise linear hypothesis used in Ref. [30], we approximate $\langle x_\tau | x, t; \cdot \rangle$ as

$$\langle x_\tau | x, t; \cdot \rangle \approx S(1, t|\cdot) x \Theta(x) + S(-1, t|\cdot) x \Theta(-x), \quad (\text{A5})$$

where $S(\sigma, t|\cdot)$, $\sigma \in \{-1, 1\}$ is independent of x , and $\Theta(\cdot)$ is the Heaviside's unit step function. This hypothesis holds in the limited situation wherein a major deformation of the effective potential (4.1) as shown in Fig. 3 is regarded as $O(x^2)$. In each of the domains, $x \leq 0$, $\langle x_\tau | x, t; \cdot \rangle$ is linearized with each of the coefficients $S(\pm 1, t|\cdot)$, which depend on the condition “dot.” This expression utilizes the symmetric property of the system.

Conversely, regarding Eq. (A5) as a definition of $S(\sigma, t|\cdot)$, $S(\sigma, t|\cdot)$ can be read as

$$S(\sigma, t|\cdot) \approx \frac{\int_{-\infty}^{\infty} dx dx_\tau x x_\tau \Theta(\sigma x) p(x, t; x_\tau, t - \tau|\cdot)}{\int_{-\infty}^{\infty} dx x^2 \Theta(\sigma x) p(x, t|\cdot)}, \quad (\text{A6})$$

from Eqs. (2.6) and (2.7). Assuming that the CPDF and the CJPDF in the integrand in Eq. (A6) have the sharp peaks near the points $x, x_\tau = \pm 1$, Eq. (A6) is replaced by

$$S(\sigma, t|\cdot) \approx \tilde{S} \sum_{\sigma_\tau} \sigma_\tau \sigma \frac{P(\sigma_\tau, t - \tau; \sigma, t|\cdot)}{P(\sigma, t|\cdot)} \quad (\text{A7})$$

with the conditional and conditional joint probabilities for the dichotomous variables, where $\sum_{\sigma_\tau} \equiv \sum_{\sigma_\tau \in \{\pm 1\}}$, and variable(s) in the additional condition(s) “dot” is(are) also replaced by the corresponding dichotomous variable(s). The constant \tilde{S} can be regarded as a number close to unity. Although it may be a useful adjustable parameter in regression analysis, we fix it as $\tilde{S} = 1$ for a simplification. By incorporating Eq. (A5) into $\Phi(x, 0)$ [= $-U(x)$] defined in Eq. (A1), we obtain

$$U(x) \equiv -\frac{V(x)}{D} - \frac{K}{2D} \{1 + S(\text{sgn}[x], t|\cdot)\} x^2 + \frac{H_{ac}(t)}{D} x, \quad (\text{A8})$$

where the constant $V(0)/D$ has been dropped.

The integrals in the transition rate (A4) can be carried out with Eq. (A8). By using the abbreviation $E_\sigma \equiv 1 - K\{1 + S(\sigma, t|\cdot)\}$, and assuming $E_\sigma/D \gg 1$, the first integral in the denominator in the right-hand side of Eq. (A4) can be estimated as

$$\begin{aligned} & \int_{x \in \mathbb{D}_{-\sigma}} dx e^{U(x)} \\ &= \int_{x \in \mathbb{D}_{-\sigma}} dx \exp \left[-\frac{x^4 - 2E_{-\sigma}x^2 + 1}{4D} + \frac{H_{ac}(t)}{D} x \right] \\ &\approx \sqrt{\frac{\pi D}{E_{-\sigma}}} \exp \left[-\frac{1 - E_{-\sigma}^2}{4D} - \sigma \frac{H_{ac}(t)\sqrt{E_{-\sigma}}}{D} \right] \end{aligned} \quad (\text{A9})$$

by the Gaussian integral approximation around the point $x = -\sigma\sqrt{E_{-\sigma}}$, where the terms of $O(h^2)$ are dropped. Likewise, keeping the terms up to $O(h)$, we obtain the second integral of the denominator in the right-hand side of Eq. (A4) as

$$\begin{aligned} & \int_{x_-}^{x_+} dx e^{-U(x)} \\ &= \int_{x_-}^0 dx \exp \left[\frac{x^4 - 2E_{-1}x^2 + 1}{4D} - \frac{H_{ac}(t)}{D} x \right] \\ &\quad + \int_0^{x_+} dx \exp \left[\frac{x^4 - 2E_1x^2 + 1}{4D} - \frac{H_{ac}(t)}{D} x \right] \\ &\approx e^{1/(4D)} \int_{-\infty}^0 dx \exp \left(-\frac{E_{-1}}{2D} x^2 \right) \left\{ 1 - \frac{H_{ac}(t)}{D} x \right\} \\ &\quad + e^{1/(4D)} \int_0^{\infty} dx \exp \left(-\frac{E_1}{2D} x^2 \right) \left\{ 1 - \frac{H_{ac}(t)}{D} x \right\} \\ &\approx e^{1/(4D)} \left[\frac{1}{2} \sqrt{\frac{2\pi D}{E_{-1}}} + \frac{H_{ac}(t)}{E_{-1}} + \frac{1}{2} \sqrt{\frac{2\pi D}{E_1}} - \frac{H_{ac}(t)}{E_1} \right] \\ &\approx e^{1/(4D)} \sqrt{\frac{2\pi D}{\bar{E}}}, \end{aligned} \quad (\text{A10})$$

where $\bar{E} \equiv 1 - K\{1 + \sum_{\sigma} S(\sigma, t|\cdot)/2\}$, and the factor $S(1, t|\cdot) - S(-1, t|\cdot)$ is regarded to be $O(h)$ [30]. From Eq. (A7), we have

$$\bar{E} = 1 - K \sum_{\sigma} \frac{P(\sigma, t - \tau; \sigma, t|\cdot)}{P(\sigma, t|\cdot)} \equiv 1 - K A_1(t|\cdot), \quad (\text{A11})$$

where $A_1(t|\cdot)$ is defined in Eq. (4.6). By substituting Eqs. (A9) and (A10) into Eq. (A4), we have

$$W(\sigma, t|\cdot) \approx \frac{\sqrt{\bar{E} E_{-\sigma}}}{\sqrt{2\pi}} \exp \left\{ -\frac{E_{-\sigma}^2}{4D} + \sigma \frac{H_{ac}(t)\sqrt{E_{-\sigma}}}{D} \right\}. \quad (\text{A12})$$

For the sake of convenience, let us define

$$B_1(t|\cdot) \equiv \frac{1}{2} \sum_{\sigma} \sigma S(\sigma, t|\cdot) = \sum_{\sigma} \sigma \frac{P(\sigma, t - \tau; \sigma, t|\cdot)}{P(\sigma, t|\cdot)}. \quad (\text{A13})$$

Using this, we have $E_\sigma = \bar{E} - \sigma K B_1(t|\cdot)$. Since $B_1(t|\cdot)$ is a quantity of $O(h)$, within the approximation up to

$O(h)$, we have $\sqrt{\bar{E}E_{-\sigma}} \approx \bar{E} + \sigma K B_1(t|\cdot)/2$, $E_{-\sigma}^2 \approx \bar{E}^2 + 2\sigma \bar{E} K B_1(t|\cdot)$, and

$$W(\sigma, t|\cdot) \approx \frac{1}{\sqrt{2\pi}} \exp\left(-\frac{\bar{E}^2}{4D}\right) \left\{ 1 - \sigma \frac{\bar{E}K}{2D} B_1(t|\cdot) + \sigma \frac{\sqrt{\bar{E}}}{D} H_{ac}(t) \right\} \left\{ \bar{E} + \sigma \frac{K}{2} B_1(t|\cdot) \right\}. \quad (A14)$$

The right-hand side of Eq. (4.4) is obtained by expanding the factors $\{\dots\} \times \{\dots\}$ in Eq. (A14) up to $O(h)$.

APPENDIX B: DELAY-COORDINATE SERIES EXPANSION

From the properties $\sum_{\sigma=\pm 1} P(\sigma, t|\cdot) = 1$ and $\sum_{\sigma'=\pm 1} P(\sigma', t'|\cdot) = P(\sigma, t|\cdot)$, we find that the function $Q(\sigma, t|\cdot) \equiv P(\sigma, t|\cdot) - 1/2$ multiplied by $A_1(t|\cdot) (\equiv A_1)$ defined in Eq. (4.6) yields

$$A_1 Q(\sigma, t|\cdot) = Q(\sigma, t|\cdot) + Q(\sigma, t - \tau|\cdot) - \frac{\sigma}{2} B_1(t|\cdot). \quad (B1)$$

This application to functions of A_1 , say $F(A_1)$, has

$$\begin{aligned} & \{F(A_1) - F(1)\} Q(\sigma, t|\cdot) \\ &= \frac{F(A_1) - F(1)}{A_1 - 1} \left\{ Q(\sigma, t - \tau|\cdot) - \frac{\sigma}{2} B_1(t|\cdot) \right\}. \end{aligned} \quad (B2)$$

For a function of A_1 , if we take $\bar{E} = 1 - KA_1$ defined in Eq. (A11), we have

$$\bar{E} Q(\sigma, t|\cdot) = (1 - K)Q - K \left(Q_\tau - \frac{\sigma}{2} B_1 \right), \quad (B3)$$

where $B_1 = B_1(t|\cdot)$, $Q \equiv Q(\sigma, t|\cdot)$, and $Q_\tau \equiv Q(\sigma, t - \tau|\cdot)$. Also, for $w_A(t|\cdot)Q(\sigma, t|\cdot)$ with $w_A(t|\cdot) (\equiv w_A)$ defined in Eq. (4.5), we obtain

$$w_A Q = w_0 Q + w_1 \left(Q_\tau - \frac{\sigma}{2} B_1 \right), \quad (B4)$$

where the coefficients $\{w_j\}_{j=0,1}$ are defined in Eqs. (4.15) and (4.16) [in Eq. (4.16), the Markov approximation described after Eq. (4.14) has been already applied to A_1]. This is the first series expansion of $w_A Q$ onto the delay-coordinate system $\{Q, Q_\tau\}$. Hereafter, the series expansion of $w_A Q$ onto the M th order delay-coordinate system $\{Q, Q_\tau, \dots, Q_{M\tau}\}$, where $Q_{M\tau} \equiv Q(\sigma, t - M\tau|\cdot)$ with a set of the expansion coefficients $\{w_j\}_{j=0}^M$, is called the M th order delay-coordinate series expansion (DCSE).

The second order DCSE is obtained as follows. The second term in Eq. (B4) is estimated as

$$w_1 Q_\tau = w_1^{(2)} Q_\tau + \frac{w_1 - w_1^{(2)}}{A_1^{(2)} - 1} (A_1^{(2)} - 1) Q_\tau \quad (B5)$$

$$= w_1^{(2)} Q_\tau + w_2^{(2)} \left(Q_{2\tau} - \frac{\sigma}{2} B_1^{(2)} \right), \quad (B6)$$

where

$$w_1^{(2)} \equiv \lim_{A_1 \rightarrow 1} w_1 = \frac{w_0 K}{2D} \left(1 - K - \frac{2D}{1 - K} \right), \quad (B7)$$

$$w_2^{(2)} \equiv \frac{w_1 - w_1^{(2)}}{A_1^{(2)} - 1}, \quad (B8)$$

$$A_1^{(2)} \equiv \sum_{\sigma} \frac{P(\sigma, t - 2\tau; \sigma, t - \tau|\cdot)}{P(\sigma, t - \tau|\cdot)} = A_1(t - \tau|\cdot), \quad (B9)$$

$$B_1^{(2)} \equiv \sum_{\sigma} \sigma \frac{P(\sigma, t - 2\tau; \sigma, t - \tau|\cdot)}{P(\sigma, t - \tau|\cdot)} = B_1(t - \tau|\cdot). \quad (B10)$$

By substituting Eq. (B6) into (B4), we have

$$w_A Q = w_0 Q + w_1^{(2)} Q_\tau + w_2^{(2)} \left(Q_{2\tau} - \frac{\sigma}{2} B_1^{(2)} \right) - \frac{\sigma w_1}{2} B_1(t|\cdot). \quad (B11)$$

Applying the Markov approximation, we replace $A_1^{(2)}$ and $B_1^{(2)}$ with $\sum_{\sigma} P(\sigma, t - 2\tau|\sigma, t - \tau)$ and $\sum_{\sigma} \sigma P(\sigma, t - 2\tau|\sigma, t - \tau)$ in addition to the same replacement for A_1 and B_1 with Eqs. (4.10) and (4.11). Also, assuming $P(\sigma, t|\sigma', t') = P(-\sigma, t \pm \tau|\sigma', t' \pm \tau)$, which comes from the symmetric property of the system [30], Eq. (B11) is approximated as

$$w_A Q \approx w_0 Q + w_1^{(2)} Q_\tau + w_2^{(2)} Q_{2\tau} - \frac{\sigma}{2} w_B B_1(t), \quad (B12)$$

where $A_1^{(2)}(t|\cdot)$ and $B_1^{(2)}(t|\cdot)$ are replaced as $A_1^{(2)}(t|\cdot) \rightarrow A_1$ and $B_1^{(2)}(t|\cdot) \rightarrow -B_1(t)$, and hence

$$w_2^{(2)} \approx \frac{w_1 - w_1^{(2)}}{A_1 - 1}, \quad (B13)$$

$$w_B \equiv w_1 - w_2^{(2)}. \quad (B14)$$

In a similar way, we may obtain more higher order series of expansion, however, the computations for the response function will be much harder. Also, we should note that the last replacements utilize the symmetric property of the system.

APPENDIX C: BACKWARD AND ADJOINT MASTER EQUATIONS

Let us obtain backward and adjoint equations from Eq. (4.12) under the Markov approximation. The Markov approximation reads Eq. (4.12) as

$$\begin{aligned} \partial_t P_*(\sigma, t|\sigma', t') &\approx W(\sigma, t) P_*(-\sigma, t|\sigma', t') \\ &\quad - W(-\sigma, t) P_*(\sigma, t|\sigma', t'), \end{aligned} \quad (C1)$$

where the transition rate $W(\sigma, t)$ is no longer conditional to “ σ', t' ,” and $P_*(\sigma, t|\sigma', t')$ ($t > t'$) represents the asymptotic conditional probability for a sufficient passage of the times t and t' . For $P_*(\sigma, t|\sigma', t')$, we impose the Chapman-Kolmogorov equality

$$P_*(\sigma, t|\sigma', t') = \sum_{\sigma''} P_*(\sigma, t|\sigma'', t'') P_*(\sigma'', t''|\sigma', t') \quad (C2)$$

for $t' < t'' < t$ and $t' > t'' > t$ [30]. Moreover, we assume

$$P_*(\sigma, t|\sigma', t') = P_*(-\sigma, t \pm \tau|\sigma', t' \pm \tau), \quad (C3)$$

from the symmetric property of the system. From Eqs. (C1) and (C2), we obtain the adjoint master equation as

$$\begin{aligned} \partial_t P_*(\sigma', t'|\sigma, t) &\approx P_*(\sigma', t'|\sigma, t) W(-\sigma, t) \\ &\quad - P_*(\sigma', t'|\sigma, t) W(-\sigma, t) \quad (t' > t). \end{aligned} \quad (C4)$$

With the asymptotic probability $P_*(\sigma, t)$ of Eq. (4.8), we impose that the asymptotic conditional probability $P_*(\sigma, t|\sigma', t')$ satisfies

$$P_*(\sigma, t|\sigma', t')P_*(\sigma', t') = P_*(\sigma', t'|\sigma, t)P_*(\sigma, t) \quad (\text{C5})$$

for $t > t'$. By applying Eq. (C5) to (C1) and (C4) with (4.8), it is found that $P_*(\sigma, t|\sigma', t')$ ($t < t'$) satisfies

$$\begin{aligned} \partial_t P_*(\sigma, t|\sigma', t') &\approx W_*(-\sigma, t)P_*(\sigma, t|\sigma', t') \\ &\quad - W_*(\sigma, t)P_*(-\sigma, t|\sigma', t') \quad (t < t'), \end{aligned} \quad (\text{C6})$$

$$\begin{aligned} \partial_t P_*(\sigma', t'|\sigma, t) &\approx P_*(\sigma', t'|\sigma, t)W_*(-\sigma, t) \\ &\quad - P_*(\sigma', t'|\sigma, t)W_*(\sigma, t) \quad (t > t'), \end{aligned} \quad (\text{C7})$$

where

$$W_*(-\sigma, t) \equiv W(\sigma, t) \frac{P_*(-\sigma, t)}{P_*(\sigma, t)} = W(-\sigma, t) + \frac{\partial_t P_*(\sigma, t)}{P_*(\sigma, t)}. \quad (\text{C8})$$

Here, let us define $\langle \sigma \rangle_t \equiv \sum_{\sigma} \sigma P_*(\sigma, t)$, then we have $P_*(\sigma, t) = (1 + \sigma \langle \sigma \rangle_t)/2$. Regarding $\langle \sigma \rangle_t$ as $O(h)$, and according to the adiabatic approximation, neglecting the terms of $O(\Omega h)$ and $O(h^2)$, from Eqs. (4.4) and (C8), we assume

$$\begin{aligned} \sum_{\sigma} W_*(\sigma, t) &\approx w_A, \\ \sum_{\sigma} \sigma W_*(\sigma, t) &\approx w_h H_{ac}(t) - w_K B_1(t) - 2\langle \dot{\sigma} \rangle_t. \end{aligned} \quad (\text{C9})$$

From Eqs. (C4), (C6), (C7), (C9), and (4.4), we obtain equations of motion for $a(t, t') \equiv \sum_{\sigma} P_*(\sigma, t|\sigma, t') - 1$ as

$$\partial_t a(t', t) \approx a(t', t)w_A(t) \quad (t' > t), \quad (\text{C10})$$

$$\partial_t a(t, t') \approx w_A(t)a(t, t') \quad (t < t'), \quad (\text{C11})$$

$$\partial_t a(t', t) \approx -a(t', t)w_A(t) \quad (t' < t). \quad (\text{C12})$$

Here, from Eq. (C2), $Q(\sigma, t|\sigma', t') \equiv P(\sigma, t|\sigma', t') - 1/2$ for $t < t'$ multiplied by $A_1(t) = \sum_{\sigma} P(\sigma, t - \tau|\sigma, t)$ yields

$$\begin{aligned} A_1(t)Q(\sigma, t|\sigma', t') &= Q(\sigma, t|\sigma', t') \\ &\quad + Q(\sigma, t - \tau|\sigma', t') - \frac{\sigma}{2}B_1(t), \end{aligned} \quad (\text{C13})$$

where $B_1(t) = \sum_{\sigma} \sigma P(\sigma, t - \tau|\sigma, t)$. This results in the same form as Eq. (B1). Consequently, $Q(\sigma, t|\sigma', t')$ has similar relations to Eqs. (B2)–(B4), and we have

$$\begin{aligned} w_A Q(\sigma, t|\cdot) &\approx w_0 Q(\sigma, t|\cdot) + w_1^{(2)} Q(\sigma, t - \tau|\cdot) \\ &\quad + w_2^{(2)} Q(\sigma, t - 2\tau|\cdot) - \frac{\sigma}{2}w_B B_1(t), \end{aligned} \quad (\text{C14})$$

for $t < t'$, where the dot abbreviates “ σ', t' ” and the coefficients w_0 , $w_1^{(2)}$, $w_2^{(2)}$, and w_B are given by Eqs. (4.15), (B7), (B13), and (B14). Then, up to the second order DCSE, we have $w_A(t)a(t, t') = \sum_{j=0}^M w_j a(t - j\tau, t')$ [$M = 1, 2$], and Eq. (4.19), with the same coefficients $\{w_j\}_{j=0}^M$ as in Eqs. (4.15) and (4.16), and the description following them.

Equation (C12) can also have a similar expansion to Eq. (C14) by virtue of the symmetry. Namely, using Eqs. (C2) and (C3), we obtain

$$\begin{aligned} a(t' - j\tau, t)A_1(t) &= a(t' - j\tau, t) \\ &\quad + a(t' - (j+1)\tau, t) \quad (j = 0, 1, \dots). \end{aligned} \quad (\text{C15})$$

This form for $j = 0$ corresponds to Eqs. (B1) and (C13) since $a(t, t') = \sum_{\sigma} Q(\sigma, t|\sigma, t')$. This, therefore, leads to $a(t', t)w_A(t) = \sum_{j=0}^M a(t' - j\tau, t)w_j$, and Eq. (4.20), with the same coefficients $\{w_j\}_{j=0}^M$ as mentioned above. However, the same expansion has not been obtained for the case Eq. (C10) from the restriction on the time ordering in Eq. (C2).

As well as Eqs. (C10)–(C12), from Eqs. (C4) and (C6)–(C9), equations of motion for $B(t, t') \equiv \sum_{\sigma} \sigma P_*(\sigma, t|\sigma, t')$ can be obtained as Eqs. (4.23)–(4.26). In Eq. (4.25), we have used the fact that $w_A B(t, t')$ for $t < t'$ can be expanded into $\sum_{j=0}^M w_j B(t - j\tau, t') - w_B B_1(t)$ [$M = 1, 2$] from Eq. (C14).

-
- [1] R. Benzi, A. Sutera, and A. Vulpiani, *J. Phys. A: Math. Gen.* **14**, L453 (1981).
 - [2] R. Benzi, G. Parisi, A. Sutera, and A. Vulpiani, *Tellus* **34**, 10 (1982).
 - [3] R. Benzi, G. Parisi, A. Sutera, and A. Vulpiani, *SIAM J Appl. Math.* **43**, 565 (1983).
 - [4] C. Nicolis, *Tellus* **34**, 1 (1982).
 - [5] B. McNamara and K. Wiesenfeld, *Phys. Rev. A* **39**, 4854 (1989).
 - [6] L. Gammaitoni, P. Hänggi, P. Jung, and F. Marchesoni, *Rev. Mod. Phys.* **70**, 223 (1998).
 - [7] A. S. Pikovsky and J. Kurths, *Phys. Rev. Lett.* **78**, 775 (1997).
 - [8] A. Neiman, P. I. Saparin, and L. Stone, *Phys. Rev. E* **56**, 270 (1997).
 - [9] J. R. Pradines, G. V. Osipov, and J. J. Collins, *Phys. Rev. E* **60**, 6407 (1999).
 - [10] B. Lindner, J. García-Ojalvo, A. Neiman, and L. Schimansky-Geier, *Phys. Rep.* **392**, 321 (2004).
 - [11] T. Ohira and Y. Sato, *Phys. Rev. Lett.* **82**, 2811 (1999).
 - [12] L. S. Tsimring and A. Pikovsky, *Phys. Rev. Lett.* **87**, 250602 (2001).
 - [13] N. B. Janson, A. G. Balanov, and E. Schöll, *Phys. Rev. Lett.* **93**, 010601 (2004).
 - [14] R. Morse and A. Longtin, *Phys. Lett. A* **359**, 640 (2006).
 - [15] G. C. Sethia, J. Kurths, and A. Sen, *Phys. Lett. A* **364**, 227 (2007).
 - [16] R. Zhu and Q. S. Li, *Phys. Lett. A* **292**, 58 (2001).
 - [17] D. Wu, X. Luo, and S. Zhu, *Phys. A (Amsterdam)* **373**, 203 (2007).
 - [18] L. Dong-Xi, X. Wei, W. Liang, and X. Yong, *Commun. Theor. Phys.* **50**, 396 (2008).
 - [19] M. Misono, T. Todo, and K. Miyakawa, *J. Phys. Soc. Jpn.* **78**, 014802 (2009).
 - [20] M. Misono and K. Miyakawa, *J. Phys. Soc. Jpn.* **79**, 034801 (2010).

- [21] K. Miyakawa, T. Tanaka, and H. Isikawa, *Phys. Rev. E* **67**, 066206 (2003).
- [22] Q. Wang, M. Perc, Z. Duan, and G. Chen, *Chaos* **19**, 023112 (2009).
- [23] Y. Jiang, *Phys. Rev. E* **71**, 057103 (2005).
- [24] T. Okano and K. Miyakawa, *Phys. Rev. E* **82**, 027202 (2010).
- [25] D. Huber and L. S. Tsimring, *Phys. Rev. Lett.* **91**, 260601 (2003).
- [26] Y. Jiang, S.-H. Dong, and M. Lozada Cassou, *Phys. Rev. E* **69**, 056225 (2004).
- [27] S. Guillouzac, I. L'Heureux, and A. Longtin, *Phys. Rev. E* **59**, 3970 (1999).
- [28] T. D. Frank, *Phys. Rev. E* **72**, 011112 (2005).
- [29] D. Wu and S. Zhu, *Phys. Lett. A* **363**, 202 (2007).
- [30] H. Tutu, *Prog. Theor. Phys.* **123**, 1 (2010).
- [31] H. Mori, *Prog. Theor. Phys.* **33**, 423 (1965).
- [32] R. Zwanzig, *Phys. Rev.* **124**, 983 (1961).
- [33] R. Kubo, *J. Phys. Soc. Jpn.* **12**, 570 (1957).
- [34] H. Nakajima and Y. Ueda, *Phys. Rev. E* **58**, 1757 (1998).
- [35] *Handbook of Chaos Control*, 2nd ed., edited by E. Schöll and H. G. Schuster (Wiley-VCH, Weinheim, 2007).
- [36] T. D. Frank, *Phys. Rev. E* **66**, 011914 (2002).
- [37] T. D. Frank, *Phys. Rev. E* **71**, 031106 (2005).
- [38] R. L. Honeycutt, *Phys. Rev. A* **45**, 600 (1992).
- [39] W. Rümelin, *SIAM J. Numer. Anal.* **19**, 604 (1982).
- [40] U. Küchler and B. Mensch, *Stoch. Stoch. Rep.* **40**, 23 (1992).
- [41] J. W. F. Brown, *Phys. Rev.* **130**, 1677 (1963).